Effect of urban microclimate on HVAC performance

Master Thesis
MSc Building Energy Design

Bendix Holtgraefe
Roland Radocz

Aalborg University
Department of The Built Environment
Thomas Manns Vej 23
DK-9220 Aalborg

Overleaf is used for typesetting the document. Adobe Illustrator 2023 and Figma are used for creating graphics. BSim is used for modeling. Python and Spyder 5.4.3 are used for data manipulation, modeling, and plotting.

Department of The Built Environment
Aalborg University
http://www.aau.dk

AALBORG UNIVERSITY
STUDENT REPORT

Title:
Effect of urban microclimate on HVAC performance

Theme:
Scientific Theme

Project Period:
Spring and Fall Semester 2023

Project Group:
-

Participant(s):
Bendix Holtgraefe
Roland Radocz

Supervisor(s):
Hicham Johra
Rasmus Lund Jensen

Copies: 1

Page Numbers: 73

Date of Completion:
January 10, 2024

Abstract:

Roof-mounted HVAC units experience vastly different temperatures than the standardized weather data typically used to dimension them. This is particularly detrimental for the cooling coil, which, as a result, can be under-dimensioned, and its annual energy demand is potentially not estimated correctly. To better understand the thermodynamic processes in the microclimate, an extensive measurement campaign has been undertaken, which revealed the impact of solar irradiation and wind speed on temperature stratification in the microclimate. Building energy simulations were then used to translate the findings into energy demand corrections for cooling coils. To allow other engineers and architects to investigate their project buildings on microclimate implications, a prediction tool has been created, which, trained on the measurement results, can indicate associated energy demand increases from placing an HVAC unit in the microclimate on roofs in Denmark. Improving the understanding of the microclimate is essential for more efficient and sustainable buildings and this thesis demonstrates how empirical data and predictive modeling can enhance architectural and engineering practices.

Contents

Preface **1**
0.1 Acknowledgements . . . 1
0.2 Reader Guide . . . 1

1 Introduction **2**
1.1 Background . . . 2
1.2 Problem statement . . . 3
1.2.1 Research Questions . . . 3
1.2.2 Delimitation . . . 3

2 Methodology **4**
2.1 Micro-climate weather station . . . 4
2.2 Data extrapolation . . . 4
2.2.1 Theories used in the extrapolation model . . . 4
2.3 Energy design analysis . . . 5

3 Measurement Results **6**
3.1 General Micro-climate observations . . . 6
3.2 Site specific micro-climate observations . . . 8
3.3 Summary of measurement results . . . 11

4 Prediction Tool **12**
4.1 Function . . . 12
4.2 Validation . . . 13
4.3 Prediction results . . . 13
4.4 Limitations . . . 15

5 Energy Demand Analysis **16**
5.1 Functional demands . . . 16
5.2 Example model . . . 16
5.2.1 Weather Data . . . 17
5.2.2 Model Types . . . 17
5.3 Model Validation . . . 17
5.4 Simulation results . . . 18
5.5 Microclimate mitigation strategies . . . 18

6 Discussion **20**
6.1 Suggestions for future work . . . 20

7 Conclusion **22**

Bibliography **23**

A Appendix - Weather Station **24**
A.1 Main Structure . . . 25
A.2 Sensors . . . 25
A.2.1 Temperature sensors . . . 25
A.2.2 Wind and solar irradiation measurements . . . 26
A.3 Micro controller . . . 26
A.4 Rain protection . . . 26
A.5 Technical Drawing of Weather Station . . . 29
A.6 Technical Drawing of 3D Printed Clamps . . . 30
A.7 Technical Drawing of Ventilated Box . . . 31
A.8 Schematic Diagram of Arduino . . . 32
A.9 Schematic Diagram of Pyranometer . . . 33

B Appendix - Measurement Period **34**
B.1 Measurement locations . . . 34
B.1.1 Location 1: TMV . . . 35
B.1.2 Location 2: PON . . . 35
B.2 Overview of sensor up-time . . . 35

C Appendix - Measurement Results **37**
C.1 Temperature sensor calibration . . . 37
C.2 Premeasurements . . . 38
C.2.1 Impact of AHU on micro-climate . . . 38
C.3 General filters applied to raw data . . . 39
C.4 Raw temperature data . . . 40
C.5 Weekly ΔT per location for the whole measurement period, daytime and peak 5% . . . 41
C.6 Full 3D mesh . . . 41
C.7 Spearman correlation analysis . . . 42

D Appendix - BSim Model **44**
D.1 Overview . . . 44
D.2 Model . . . 44
D.3 Systems . . . 47
D.4 Results . . . 50

E Appendix - Prediction tool **59**
E.1 Data filters . . . 59
E.1.1 Wind profile adjustment . . . 59
E.2 Files used for tool . . . 59
E.3 Selection of Model . . . 60
E.3.1 Equations used in regression . . . 60
E.4 Prediction tool python code . . . 61
E.5 Assumptions to use the prediction tool . . . 64

F Appendix - Prediction Tool user guide **66**

G Appendix - Arduino Code **68**
G.1 Libraries used . . . 68
G.2 Constants . . . 68
G.3 Initialization and setup . . . 68
G.4 Main program logic and data logging . . . 69
G.5 Arduino code . . . 69

H Appendix - EnviMet **72**

Preface

This report is produced as a part of the MSc Building Energy Design curriculum to complete the education at Aalborg University. This Master Thesis is worth 45 ECTS (1 ECTS = 27.5 hours), resulting in 1,237.5 hours of project time during the spring and autumn semesters of 2023 per project member.

0.1 Acknowledgements

We thank our supervisors, Hicham Johra and Rasmus Lund Jensen, for their guidance and support throughout this project. We also extend our gratitude to the laboratory staff for their assistance during the construction of the weather station.

0.2 Reader Guide

This report consists of two parts:

- Part 1: Main Report
- Part 2: Appendix with supplementing illustrations, drawings, plots, code and more detailed descriptions of methods used.

Report Structure	Appendix Structure
1	A
1.1	A.1
Table 1.1	Table A.1
Figure 1.1	Figure A.1

Aalborg University, January 10, 2024

Bendix Holtgraefe
bholtg21@student.aau.dk

Roland Radocz
rradoc21@student.aau.dk

Chapter 1

Introduction

1.1 Background

A well-established method among building engineers and architects is the utilization of weather and climate data in their design process to ensure that buildings are designed according to the prevalent climate at their geographical location. This weather and climate data is used to simulate various aspects of the building, from structural loads to the annual heat balance, and it aids the continuous decision-making that engineers are confronted with throughout the design phase. In Denmark, the weather data used for indoor climate calculations is from a standardized Design Reference Year (DRY) weather file based on measurements from the Danish Meteorological Institute (DMI) and is binding to such an extent that it is required for the energy performance calculations to gain a building permit. The weather file is the aggregate of measurements from five to six different locations across the country, spanning a total of 10 years, which are manually stitched together to create an average year of weather data applicable to the whole of Denmark. [5] [9]

The meteorological weather stations that provide the data for the data set, operate according to the World Meteorological Organization, which prescribes ground-based temperature sensors to be located at a height of two meters above the ground, equipped with a radiation screen and protected from precipitation, which reduces the impact of long-wave radiation from surrounding structures [6]. While this temperature data is sufficient for most energy calculations like transmission losses where the building envelope is in contact with the largely unaffected ambient air, in other use cases where temperatures differ heavily from the ambient temperatures, a potentially significant error is introduced to the calculations.

One field of study related to building energy where the ambient temperature has repeatedly been found to be vastly different from true air temperature, is the urban microclimate. Existing research often applies the term micro-climate to cover the area of an entire city, studying how the climate changes between its boundaries and the rural land surrounding it. Taking aspects such as the urban heat island effect and materials with a low albedo into account, temperature deviations of multiple °C can be observed between cities and their surroundings [1], yet this scale still neglects a lot of thermodynamic nuances of microclimates on even smaller scales.

Scales smaller than a city or a district have seldom been assessed when examining micro-climates, yet significant temperature gradients on a scale of just a few meters have been observed [2]. This is specifically applicable to dark surfaces like asphalt on roads or bitumen on roofs due to the low albedos of the respective material. Convection heats the closest air layers in direct proximity to these surfaces, creating an unstable temperature gradient. This scale of micro-climate has largely been overlooked in research, yet it is on this scale that crucial supply systems can be located. Notably, the ventilation unit, or at least the air intake, is sometimes placed on the roof of buildings due to space restrictions, but standard building energy modeling software does not account for the impact of this micro-climate.[4].

With always-increasing energy frame requirements in Denmark, the risk of overheating in buildings also becomes more prevalent, leading to more frequent use of cooling coils in HVAC units [8]. The energy demand of these devices is directly linked to the temperature of the inlet air they receive, where the abnormal temperatures in microclimate potentially impact the efficiency of cooling coils. Understanding the magnitude at which environmental parameters impact the actual temperatures in the first two meters above the roof surface is crucial to calculating and judging the designs of structures within this zone. To overcome this, a solid foundation of empirical data from the urban micro-climate on top of flat roofs must be collected. With empirical data as a foundation, a standardized method can be developed, which helps engineers correct the energy demand of roof-mounted ventilation units and allows

them to make nuanced design decisions when working within the microclimate.

This project aims to significantly expand upon the collection of microclimate data on the most common type of roofs found in Denmark and to create a proof of concept on how this data can be used to correct the energy demands of cooling coils in ventilation units for a given microclimate.

1.2 Problem statement

Due to the complex nature of construction projects, a building ventilation system may occasionally be placed on top of flat roofs, which exposes them to yet relatively unexplored microclimate conditions, which may introduce substantial variations to the temperatures it experiences compared to the standardized weather data used in building energy calculations. This discrepancy between the standardized weather data used and the actual characteristics of microclimates on top of dark flat roofs in urban areas potentially introduces an error to the building energy calculation process, leading to ventilation systems not appropriately designed for a given environment. This results in inefficient use of resources and a potentially less sustainable building. To mitigate this uncertainty, extensive empirical data needs to be collected and analyzed, resulting in the following research objective:

How can empirical data and predictive modeling be utilized to accurately incorporate micro-climatic conditions of flat roofs into ventilation design and energy consumption calculations?

1.2.1 Research Questions

Breaking down the problem statement into its individual components, the following research objective emerges which will be addressed in this report:

- How do environmental factors influence an urban local micro-climate system?
- How can empirical micro-climate data be extrapolated to predict micro-climates?
- How does the microclimate affect the annual energy consumption and peak loads of HVAC units placed within the microclimate?
- How can engineers incorporate these results into their design and energy calculation practices?

1.2.2 Delimitation

To answer the research questions, the project will consist of a practical and theoretical component, the scopes of which will be explained in the following section. A measurement campaign will be undertaken to understand the local urban micro-climate conditions experienced on top of dark flat roofs. This campaign is limited to locations in Aalborg, Denmark, between early July and late November of 2023 due to the time frame of the master thesis. Due to the nature of the problem statement, only flat, accessible roofs with bitumen covering will be considered prospects for installing microclimate weather stations. The recorded environmental parameters during the measurement campaign are limited to the temperature gradient of 50 to 2000 millimeters above the roof surface and pyranometer and anemometer readings for direct solar irradiance and wind speed, respectively. The placement of the measurement devices for long-term measurements is limited to the properties of Aalborg University due to the associated administrative and logistical hurdles of placing weather stations on third-party roofs. Reference data sets to extrapolate the findings of the measurement campaign will be limited to DRY weather files of 2010.

To allow other engineers to use the findings of this study, a tool will be made available that processes the empirical data and applies the relations of environmental properties to other roofs. The prediction model will be based on a black-box approach, meaning that the relations between the parameters will not follow known physical principles but instead mathematical abstract ties. The inherent weakness of these models is that they cannot deal with changes to the boundary conditions they haven't been trained for. This means that the model used in this project will only apply to predictions for buildings with characteristics matching those of the case buildings.

The extraction of ventilation unit performance parameters will be done through the use of a Denmark-specific indoor environment simulation software called BSim. Due to limitations within the software, other software may be more suitable for this application. It is at the engineer's discretion to choose the most suitable software when replicating the analyses of this study.

Chapter 2

Methodology

Empirical data collection will be emphasized during this project to improve the understanding of thermodynamic processes in micro-climates on top of flat roofs. This data will then be used to assess the influence of the microclimate on the performance and design parameters of roof-mounted ventilation units according to the methods outlined in this chapter.

2.1 Micro-climate weather station

The microclimate will be recorded using a custom weather station, equipped with a total of eight temperature sensors, which will be used to map the vertical temperature stratification, as well as a pyranometer and anemometer for measuring the direct solar radiation and wind speeds. The weather station's construction and operation details can be found in Appendix A, with the microcontroller code provided in Appendix G. The weather stations will be employed for a 4.5-month period from July to November 2023, spanning two roofs on the Aalborg University campus in Denmark. The recorded data will then be used to gain a general overview of how environmental parameters interact with each other within the micro-climate on roofs, with a particular focus being placed on "ΔT", or the temperature difference between the ambient temperature, and the temperature at a specific height above the roof surface within the micro-climate zone.

2.2 Data extrapolation

Once the environmental parameters and temperature stratification data have been recorded, a regression model will model the relations between the environmental parameters and the resulting temperature difference. The exact model used the method behind using the recorded data for predicting temperatures in the microclimate are elaborated in Appendix E. The tool aims to provide predictions for temperatures at various heights within the micro-climate. The validation of the model will be done against measured data that has not been included in the training data, and the mean absolute error across all known heights will be used to judge it.

2.2.1 Theories used in the extrapolation model

The following theories have been applied to the model to allow customization of the model to the user's case building. These customization methods imply that all assumptions explained in Appendix E are fulfilled.

Reference weather data

In Denmark, the DRY weather files have been created to function as a standardized weather file for all energy demand and indoor environmental calculations needed to obtain a building permit. While it is based on recorded data from a 10-year time frame, it has been artificially modified to represent a "normal year" across all parts of Denmark. Since this weather data is used in all other aspects of Denmark's energy and indoor environment calculations, it will also function as the base reference weather data for predictions and calculations made in this project.

Wind Profiles

While the ambient temperature and solar irradiation can be assumed to be unrelated to the geometry of the building and its surrounding structures (considering the inspected micro-climate location is not being shaded), the site-specific wind speed can be mathematically adjusted to represent local conditions by defining the surrounding characteristics and building height. For this, the wind profile power law will be used as shown in Equation 2.1

$$V_{new} = V_{ref} \cdot \frac{\ln\left(\frac{h_{new}}{z_{0,new}}\right)}{\ln\left(\frac{h_{ref}}{z_{0,ref}}\right)} \tag{2.1}$$

where:

- V_{new} is the wind speed at the new height.
- V_{ref} is the reference wind speed measured at reference height.
- h_{new} is the new height for which the wind speed is being adjusted.
- $z_{0,new}$ is the roughness length of the site at the new height.
- h_{ref} is the reference height at which the wind speed is measured.
- $z_{0,ref}$ is the reference roughness length at the reference height.

In this model, the reference wind speed (V_{ref}) from the DRY weather file will be used and adjusted through the reference height (h_{ref}) (10 meters), along with the roughness lengths ($z_{0,ref}$) (0,3 meters). $z_{0,new}$, and h_{new} will be inputs of the user based on their site specifications.

2.3 Energy design analysis

Within this project's scope, the preferred tool for analyzing the impact of micro-climates on the demands of a roof-mounted ventilation unit is "BSim". The specific simulation setup and specification, as well as instruction on how to apply the same idea to any other model, will be elaborated in Appendix D. The parameters to be analyzed are the annual energy demand for cooling and the dimension giving peak loads for cooling coils.

Chapter 3

Measurement Results

This chapter describes the results of the measurement campaign that has been undertaken to collect empirical data for the urban micro-climate on two different roofs. Further information about the selected roofs can be found in Appendix B. The investigated parameters are the vertical temperature gradient with eight temperature sensors within a 2-meter column, as well as wind speed and solar irradiation data. Measurements have been taken for a total of 142 days between July 11th 2023 and November 28th 2023. The exact uptime of sensors is shown in Appendix B

Before the main measurements, a pre-measurement has been undertaken to determine the optimal placement of measurement equipment. Specifically, the impact of ventilation units themselves on the micro-climate has been investigated. After isolating these parameters in a test setup, a significant impact has been found from the presence of a ventilation unit in the microclimate during sunny hours, which increases the overall temperature due to providing additional heat capacity, reflective surfaces, and wind protection to the areas in its direct vicinity. Detailed results of the pre-measurement can be found in Appendix C

The main measurements aim to create a thorough understanding of the urban micro-climate on roofs by measuring roofs with two different wind exposure conditions. Next to the differences in wind exposure the two buildings also have different heights, which needs to be considered in further analyses. The specific building characteristics of the two sites can be seen in Table 3.1.

Table 3.1: Placement criteria for weather station placement for main measurements.

	Roof 1 (PON)	**Roof 2 (TMV)**
Location	Aalborg, Denmark	Aalborg, Denmark
Height	4.5m	17m
Wind exposure	Moderate	High
Roughness length	1 meter	0.3 meter
Shading	None	None
Proximity to HVAC unit?	70 cm	N/A

For data treatment principles for analyses in this chapter, see Appendix C.

3.1 General Micro-climate observations

First, the recorded temperature data will be presented to gain an overall understanding of temperature stratification on flat bitumen roofs. The general temperature stratification trend is evident when looking at 1 hour of a standard summer day with high solar irradiation and low wind speeds in Figure 3.1. The measurement at 200 cm above the roof surface aligns with DMI measurements of the same period from a weather station approximately 12 kilometers from the measurement site, and the average temperature in the lower laying sensors continuously increases to a maximum right above the roof surface.

Figure 3.1: Visualization of temperature stratification on Aug. 2nd 2023 between 13:00 - 14:00 with DMI temperature as reference for PON. Shaded area = std/2; Gray dashed line = std

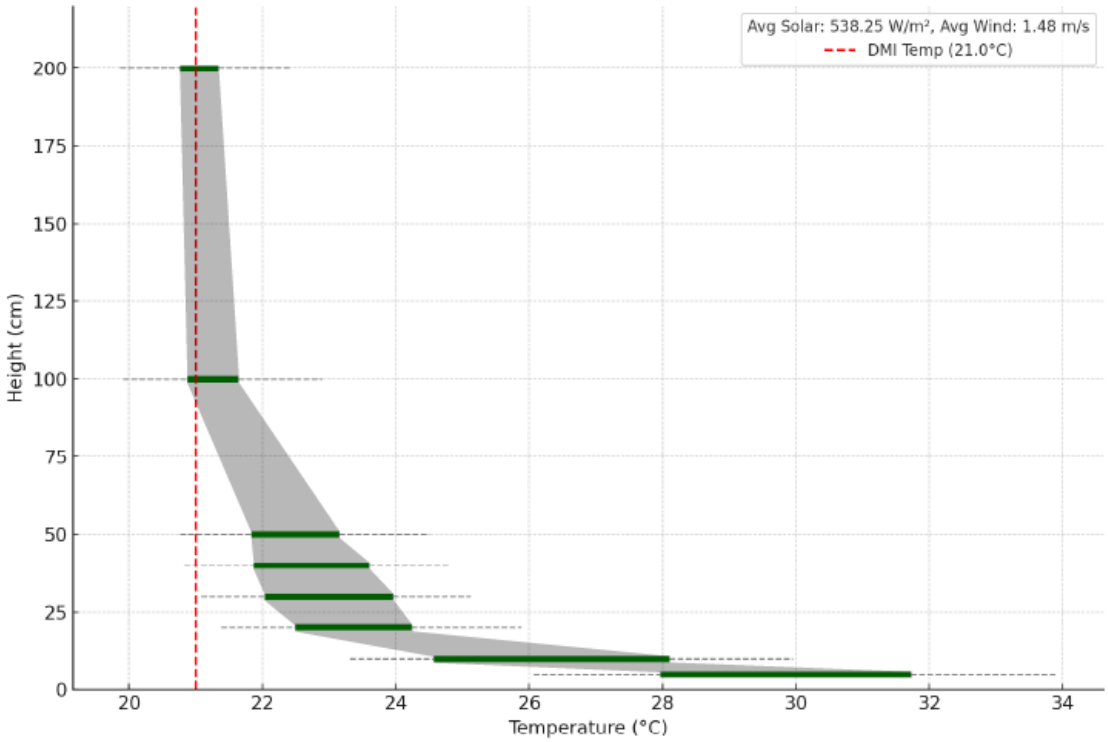

Further observations are that due to the high sampling rate of 4 seconds, there is a significant variance of temperatures for every channel, with increased volatility closer to the roof surface. The largest temperature stratification occures within the first 20cm and it gradually become more uniform as the distance from the roof surface increases. The above example shows the temperature stratification during a very sunny period with low wind speeds. Comparing this period with other days of extreme weather conditions reveals the overall principle of the interplay between the three parameters. The 4 scenarios shown in Table 3.2 represent chosen days according to the following criteria:

Table 3.2: Overview of extreme day scenarios

	Criteria 1	**Criteria 2**
Scenario 1	High Wind	Low Solar
Scenario 2	Low Wind	Low Solar
Scenario 3	High Wind	High Solar
Scenario 4	Low Wind	High Solar

Looking at the selected extreme days in Figure 3.2, the resulting ΔT between channel 8 (200 cm from roof) and channel 1 (5 cm from roof) at different wind and solar irradiation conditions shows, that solar irradiation is required for temperature stratification to occur, while increased wind speeds have a reverse effect on ΔT.

Figure 3.2: Four selected extreme days with either solar or wind at an extreme level, neither at high levels, or both at high levels. Data from PON

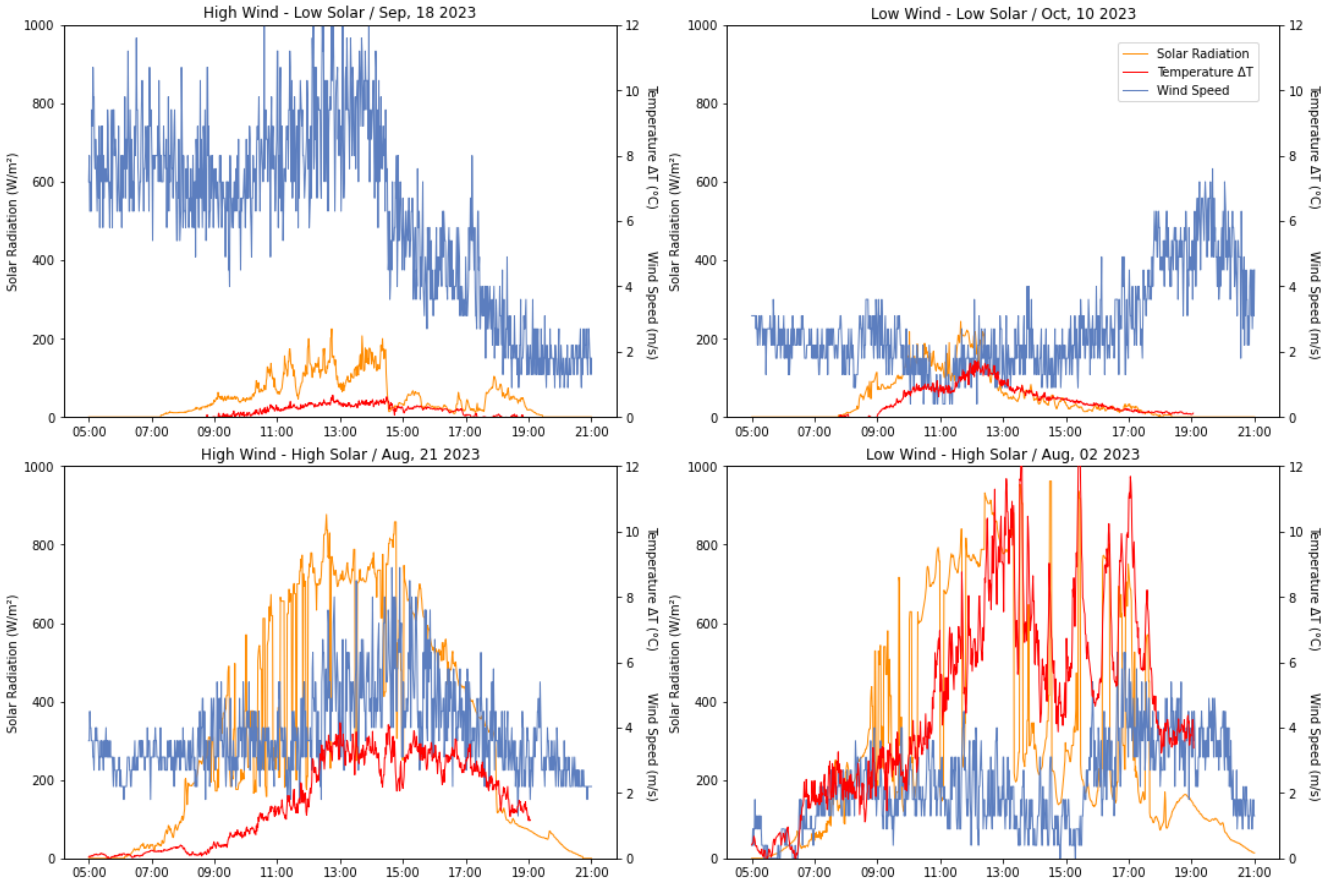

During periods of high solar irradiation and wind speeds of 1-2 m/s, ΔT spikes of up to 12°C can occur, while there is virtually no temperature gradient during times of high wind speeds or low solar irradiation. The above observations are based on data from PON, which is the more wind-shielded location. The same patterns and general relations between the three parameters of wind, solar irradiation, and the ΔT can be observed in both locations. However, the wind speed's intensity varies significantly due to different exposure levels, resulting in a generally lower ΔT at TMV.

3.2 Site specific micro-climate observations

To further improve the understanding of the micro-climate, the two case sites will be analyzed, covering aggregated data from the entire measurement period and focusing on the recorded temperature stratification under different environmental conditions. For these analyses, the temperature difference between Ch. 1 (5 cm) and Ch. 8 (200 cm) will be used as it is expected to have the strongest temperature gradient, resulting in better visualization of patterns in the data. Firstly, the different wind conditions must be considered as they significantly reduce temperature stratification.

Figure 3.3: Comparison of wind speeds between PON and TMV roof with logarithmic wind profile correction based on building heights and roughness lengths as explained in 2.1. PON data was recorded at a 4-second interval and averaged to minute data, while TMV data was recorded in minute values.

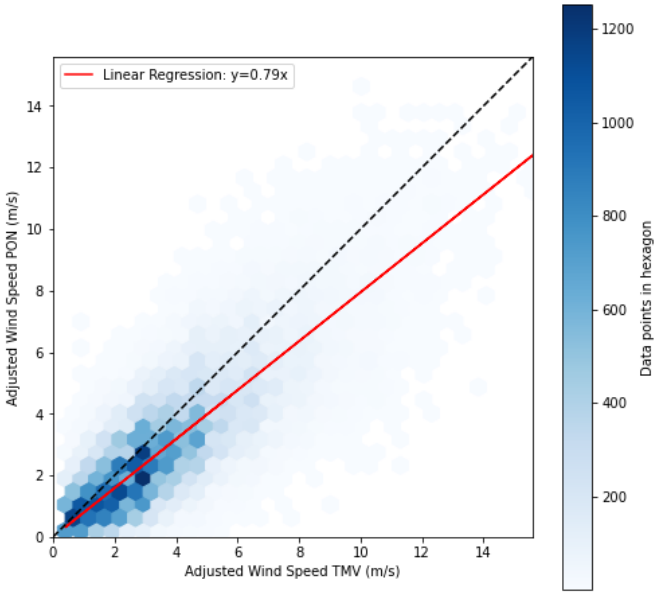

The wind speeds in Figure 3.3 have been corrected for their wind profiles, but despite this, TMV experiences a roughly 20% higher wind speed than PON. When looking at the temperature difference between the lowest and highest sensor in Figure 3.4, the impact of this difference on wind speeds becomes apparent with PON recording a higher temperature despite both sites being exposed to the same solar irradiation. This, however, only occurs during sunny periods—more cloudy conditions cause the temperature difference to be relatively equal.

Figure 3.4: Weekly average temperature difference between 8am and 6pm for Ch. 1 - Ch. 8 (5 cm - 200 cm) for both measurement locations, with weekly average solar irradiation with the same time series filters applied.

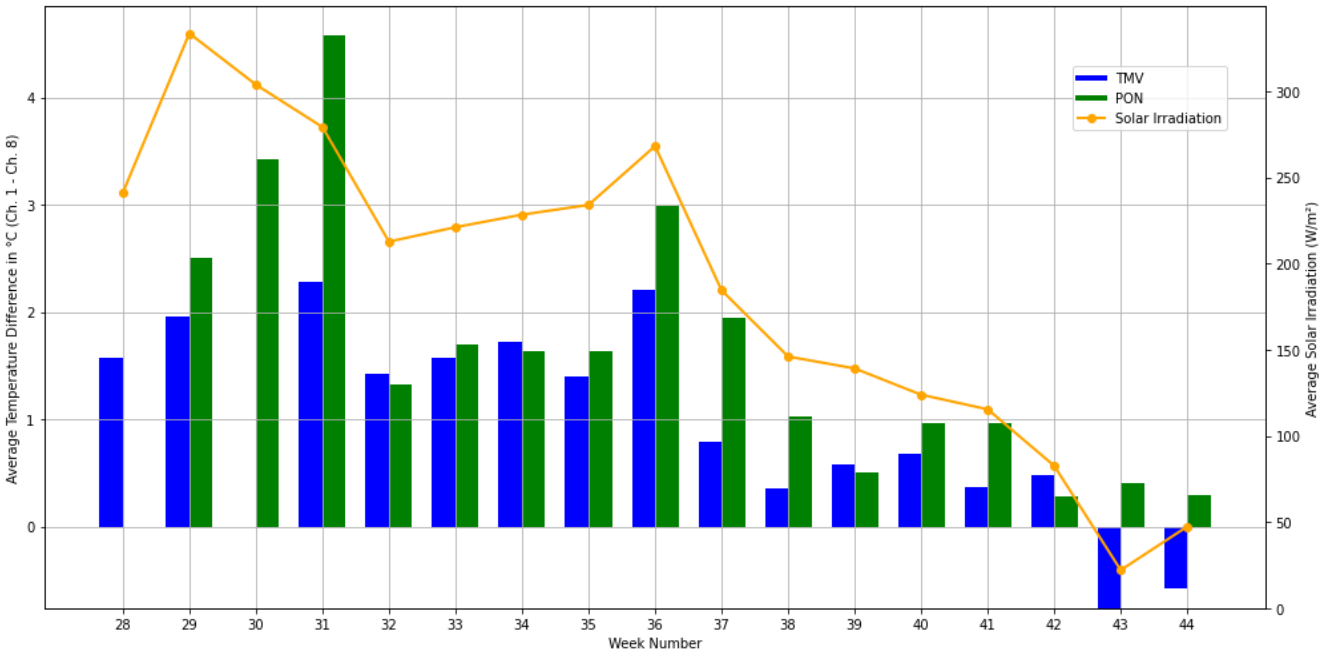

Combining the wind speed and solar irradiation as factors of ΔT for a longer period than during the extreme

day observations, the trend noticed previously becomes even more apparent. In Figure 3.5, one of the environmental parameters has been compared against ΔT, with the other parameter grouped into categories of low, medium, and high presence.

Figure 3.5: Relation between solar irradiance, wind speed and ΔT of Ch. 1 - Ch. 8 (5 cm - 200 cm) at PON (upper row) and TMV (lower row).

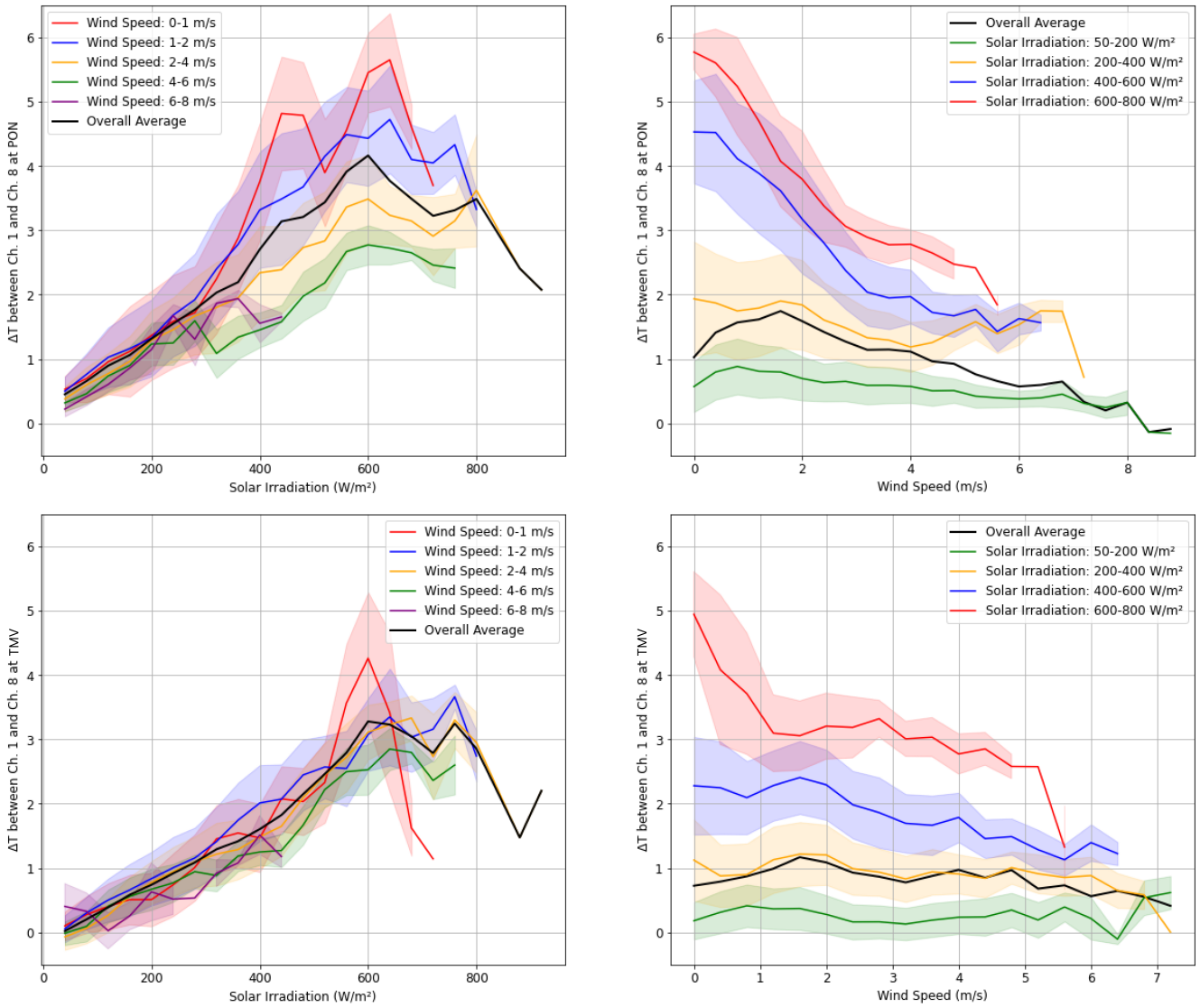

Most notably, all relations between the environmental parameters and ΔT are of an almost linear nature, while clear differences between the impact of solar irradiation and wind speed can be drawn. Solar irradiation appears to be the leading variable in determining the ΔT since especially in the range until 300 W/m^2 for PON and 550 W/m^2 for TMV, the increase of ΔT is almost independent of the wind speed. After these limits, lower wind speeds, especially at PON, result in a more significant increase of ΔT, possibly due to the roof's geometry, with several structures obstructing the airflow, especially at lower heights above the roof. For the plots with ΔT as a function of wind speed on the right side, a very different picture is drawn, with the impact of wind speed being heavily dependent on the presence of solar irradiation. As already observed with solar as a function of ΔT, the wind speed only takes effect in reducing the slope above a solar irradiation of 400 W/m^2 for PON and 600 W/m^2 for TMV. Below these thresholds, the ΔT stays almost unaffected by the wind speed.

3.3 Summary of measurement results

In conclusion of the impact of environmental variables, solar irradiation can be determined as the leading factor for determining the ΔT, while the wind speed takes a secondary role, correcting the temperature difference, but only during high solar irradiance. This principle will function as the basis for predicting ΔT on other roofs. Regarding the typical ΔT values found during the measurement campaign, which in the end impact the effectiveness of the cooling coil, the focus should be placed upon summer measurements from July (the start of the measurement period) till the end of September. The key ΔT values are summarized in Figure 3.6, showcasing the "overall" dataset, which is unfiltered regarding the time of the measurement; the daytime dataset, which is filtered for hours between 08:00 and 18:00, where the cooling coil is expected to be used for standard office hours, and the peak 5% temperatures which are important for determining the change to peak loads of the cooling coil.

Figure 3.6: Overview of average ΔT across all channels from aggregated PON and TMV data for three categories. Datatable of key results below. Complete data table with weekly averages per channel can be found in Appendix C

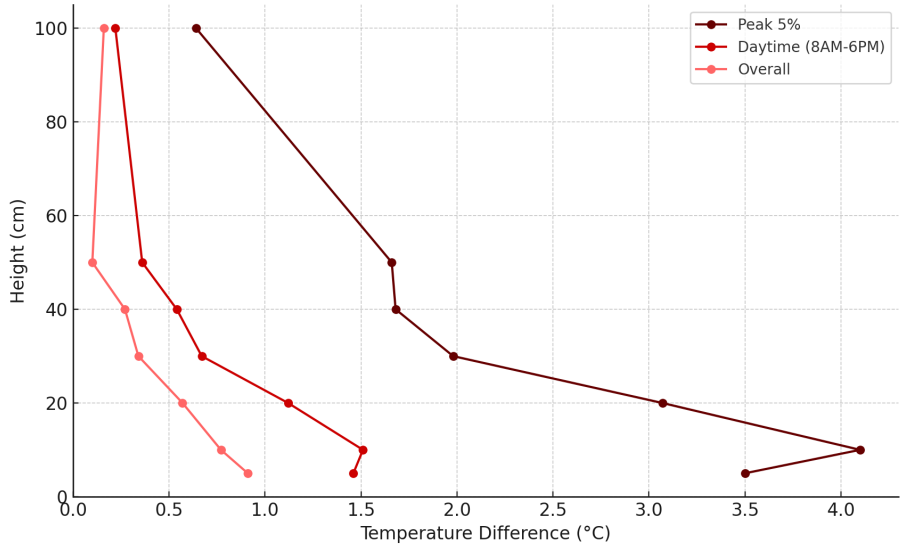

Height	Overall	Daytime (8AM-6PM)	Peak 5%
5 cm	0.91	1.46	3.50
30 cm	0.34	0.67	1.98
50 cm	0.10	0.36	1.66

In the context of the used weather station, the 5 cm measurement represents the measurement closest to the ground and, therefore, is theoretically the most impacted by convection from the roof surface heating the air in the microclimate. During daytime hours when a cooling coil would typically be operated, the average ΔT is found to be 1.46°C, which can significantly impact the energy demand for cooling. Since this is a mean value across a timeframe of eleven weeks, peaks on warm summer days are even higher, which is also when cooling coils are used the most. The heights 30 cm and 50 cm have been chosen as key values since they cover the range at which inlet ducts of roof-mounted ventilation units are commonly positioned. These heights already show a significant reduction in ΔT of more than 50% and 75% compared to 5 cm. While the drop is substantial, it may still noticeably impact the energy demand.

In the next sections of this report, these conclusions will be applied to model the prediction tool, which allows the application of the microclimate analysis onto other roofs, and the resulting ΔT summarized in Figure 3.6 will be used to calibrate the building energy simulation model, which will then return the impact on the cooling coil.

Chapter 4

Prediction Tool

The ΔT found for this project's case buildings in Table 3.6 is a product of the exact weather that occurred during the measurement period, with the specific building geometry and surroundings also playing a role. To make the results transferable to other buildings so that other engineers can make use of the insights for their own projects, the pattern between the variables of solar irradiation, wind speed, and temperature needs to be numerically approximated, building-specific parameters need to be accounted for, and the underlying weather data needs to be generalized. For this purpose, a tool has been developed, which allows engineers and architects to apply the principle of microclimate stratification to their case buildings. Ideally, this would be done in a white box model, which accurately models the real thermodynamic processes of the microclimate. Due to the complexity of such models, a more straightforward black box approach has been chosen, which, through regression modeling of the relations found during the measurements and presented in 3.2 predicts microclimate temperatures in various settings.

In this chapter, the basic principle of this regression model will be elaborated, with an overview of how the model has been tested and validated. Lastly, some example results of the tool will be presented, which will be used in the next step to determine the energy demand impact of the microclimate predicted here.

4.1 Function

Fundamentally, a linear regression model approach has been chosen as the relationships between solar irradiation, wind speed, and the temperature stratification identified in Figure 3.5 are primarily linear. The solar irradiation has been determined as the leading factor for the temperature stratification, meaning that it receives a higher weight in the linear regression. In the final application of the model, all available valid data from the measurements from both locations have been combined and used as training data. An individual regression model for every one of the microclimate temperature channels is created, fitting it to the training data to reduce the mean error across the dataset. To achieve this, the model has been fitted for solar irradiation and wind speed, and a final coefficient has been added to remove any mean error. To account for the different wind profiles at the two locations, which are at vastly different heights and exposure levels, as well as to allow comparison of the measured data to 3$^{\text{rd}}$ party roofs, the recorded wind speeds have been adjusted to the wind profile through the use of the logarithmic wind profile Equation 2.1. A detailed description of the data filters used, the wind profile adjustment, the final regression equations and the code for the tool are provided in Appendix E. A detailed user guide on how to use the tool for other roofs is provided in Appendix F.

The final linear regression Equation 4.1 has been used for modeling with a main linear term describing the relation between ΔT and solar irradiation. Further, the impact of wind has been corrected with a second linear wind-related term, and the mean error per channel has been corrected with the constant "c".

$$\Delta T_{Ch} = a \cdot Solar + b \cdot Wind + c \tag{4.1}$$

Where:

- ΔT: Temperature difference between the channel and the ambient temperature in °C
- $Solar$: Solar radiation in W/m^2
- $Wind$: Adjusted wind speed in $°C$

And the coefficients a, b, c represent:

- a: Coefficient for solar irradiation.
- b: Coefficient for wind speed.
- c: Channel-specific constant, correcting for mean error.

The model is trained on the measured data presented in Appendix C and the resulting models are then fed with weather data in the form of DRY 2010 weather data. To apply the tool to other climates, the weather data needs to be exchanged with different local or nationally standardized weather data sets. The model is only trained on heights where temperature sensors were installed for the weather stations. To also allow for predictions of temperatures between the known channels, in-between heights will be determined based on polynomial interpolation from the surrounding channels. User-specific inputs for the roughness length and building height in question will be made available, and the wind speed of the base weather file will be adjusted accordingly. With the temperature differences predicted at various heights in the microclimate, these temperatures will then be converted to potential energy demand impacts for the annual energy demand or peak loads of cooling coils in roof-mounted ventilation units.

4.2 Validation

During the fitting of the models, 20% of the raw data has been used for testing the resulting equations. The mean absolute error (MAE) is the main performance indicator for the accuracy of the models. The mean error has been nullified when fitting the c-constant. Table 4.1 shows the MAE for each channel, based on 20% of the dataset acting as testing data with randomized samples from across the dataset.

Table 4.1: Mean error at different channels for TMV and PON.

	Height (cm)	**MAE (°C)**	**Mean Error (°C)**
Ch. 1	5	0.43	-0.0
Ch. 2	10	0.45	-0.01
Ch. 3	20	0.45	-0.01
Ch. 4	30	0.37	-0.01
Ch. 5	40	0.27	-0.0
Ch. 6	50	0.34	-0.0
Ch. 7	100	0.21	0.0

Lower channels show a higher mean error which can be drawn back to generally higher temperature fluctuations right above the roof. As the distance to the roof surface increases, the MAE decreases as well. A MAE below 0.5°C is found to be acceptable considering the standard deviation of measurements of multiple °C as shown in Figure 3.1 and Figure 3.5, and considering the variance of temperatures between sensors found during calibration (see Appendix B).

4.3 Prediction results

To showcase the general predictive capabilities, the model has been applied to an arbitrary roof, simulating the daytime hours of the summer period from June to September. Figure 4.1 shows that the same trends as in the exemplary day shown in Figure 3.1 can be observed with stronger temperature stratification for the lower channels and a gradually decreasing temperature difference for the upper channels.

Figure 4.1: Predicted temperatures for each channel with DRY2010 as base weather file. Predictions are mean temperatures for the summer months with time filters limiting it to datapoints between 08:00 and 18:00. Green band showing the MAE from Table4.1; Dashed line shows ±10% range of data points

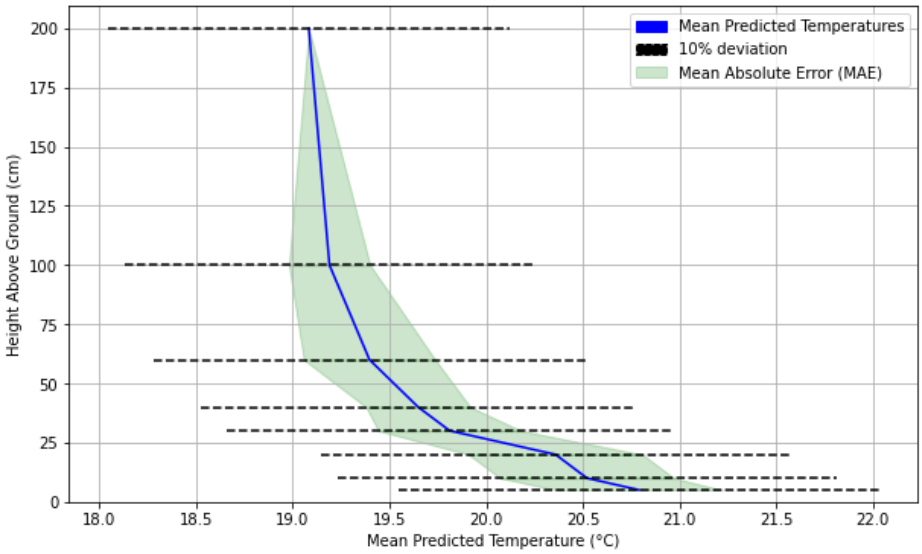

Since the plot is based on a significantly larger data set compared to the exemplary day, the stratification has significantly smaller extremes. Additionally, despite correcting the wind speed for the case-specific wind exposure, the DRY 2010 weather data file has a significantly higher mean wind speed, resulting in generally lower observed ΔT.

The above plot is subject to the wind speed correction of the chosen building parameters. These can be replaced by the users with case-specific parameters. The magnitude of hypothetical changes to these parameters is shown in Figure 4.2, where different building heights and roughness lengths are compared.

Figure 4.2: Comparison of the impact of changing wind speed related site-specific parameters (Roughness length "r" and building height "h") with all filters from Figure 4.1 applied.

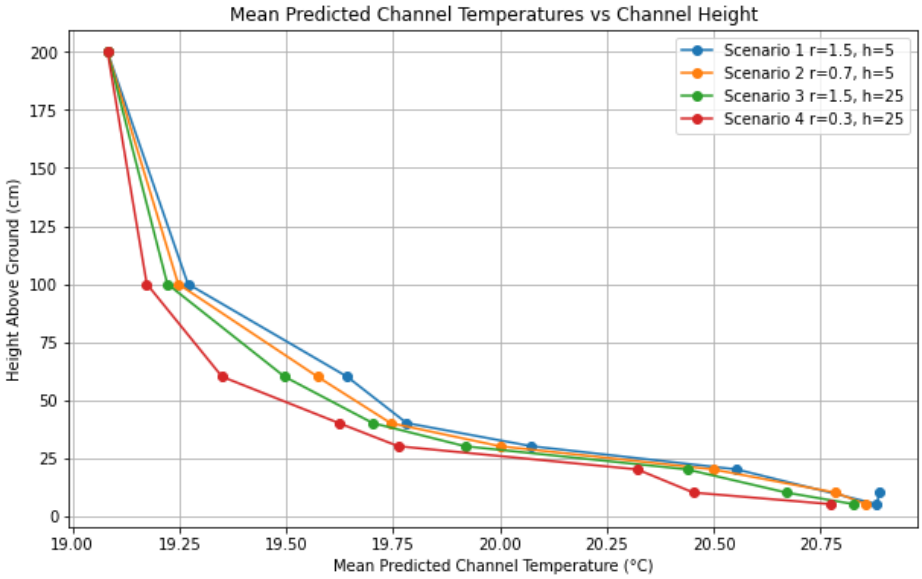

Clear trends resulting from the changed building parameters can be observed, with taller (higher "h") and less exposed (smaller "r") buildings experiencing higher wind speeds and, therefore, narrower temperature gradients. The above predictions of the model act as a proof of concept. Before the results are used for design decisions,

case-specific customization of the tool needs to be made. A detailed description of how the tool functions and how to customize the tool for other buildings is explained in Appendix F.

4.4 Limitations

The tool can predict temperatures at different heights in the microclimate with acceptable MAE margins, as shown in Table 4.1. Still, there are significant limitations to using the tool when attempting to apply it to other roofs. Firstly, all training data is based on a measurement campaign done on roofs with a black bitumen surface, meaning that other roof surfaces with other albedos would result in different patterns. Further, all measurements were taken in locations without natural shading from surrounding structures. If predictions are made for sites with partial shading on the HVAC unit inlet, the tool will not be able to account for this. The model has only been trained on environmental parameters of solar irradiation, wind speed, and ambient temperature. Factors such as relative humidity or wind direction have not been considered but can also physically impact the microclimate. Lastly, the roof's geometry and peripheral strictures can impact the experienced wind speed on roofs, which can not be accounted for by the roughness length. If the target roof layout significantly differs from the rather open roofs of the measurement campaign, the accuracy of predictions may be substantially reduced. Roof layouts are described in Appendix B.

Chapter 5

Energy Demand Analysis

After determining the temperature difference at a specified height in the microclimate zone, the resulting impact on a cooling coil can be determined. For this, an energy simulation model must be created, which allows the isolation of the inlet temperature variable. Different indoor environment simulation programs can be used for this purpose if they fulfill the functional demands outlined below. In the context of this project, the software "BSim" has been utilized, which is the standard in Denmark for indoor environment and building energy design simulations. The following chapter describes the principle upon which the energy demand analysis has been conducted to allow replications for other case buildings. The models used in this analysis are of exemplary nature and do not represent actual buildings.

5.1 Functional demands

The main functional demand of the energy demand analysis model is the ability to isolate the ventilation inlet temperature as a variable, which then mimics the temperature changes in the microclimate. Further, the software must be capable of calculating the resulting energy demand of cooling coils of ventilation units, as well as their peak load capacity.

5.2 Example model

Ideally, the microclimate temperature resulting from the prediction tool is directly applied to the inlet air temperature. This way, the impact can be assessed with the highest accuracy. In the case of this project, which utilizes BSim, this was not available, so the following workaround has been made:

An example room has been created, representing a typical office. To mimic the microclimate, a source room has been created with properties that react to environmental changes in a similar manner as an open space on a roof would, with the variables shown in Table 5.1 being tweaked until the thermal behavior of a microclimate on a roof has been replicated.

Table 5.1: Source room properties to replicate microclimate on roofs.

Component	**Properties**	**Effect**
Skylight	size, g-value	Passive solar gain to replicate impact of solar irradiation.
Window (South Wall)	size, g-value	Passive solar gain to replicate impact of solar irradiation.
Infiltration	Air change rate	Replicates impact of wind.
Envelope	Thickness, Transmission	Heat capacity of envelope determines the latency of temperature decrease after environmental parameters have changed.

This source room is then selected as the source of the ventilation system for the target room. A detailed description of the model with the setup and parameters of the source room, as well as the ventilation principle and assumed loads of the target room are explained in Appendix D.

5.2.1 Weather Data

The weather data in BSim is sourced from DRY files. This is compatible with the predicted microclimate temperature from the tool, which uses the same DRY weather data as input to make predictions. Simulations have also been run with future expected weather data from the DRY 2050 weather file, but the results have been deemed unusable. The wind speed in that file is approximately twice as high as for the 2010 weather data which heavily reduces all ΔT predictions and doesn't add value to the analyses of this research.

5.2.2 Model Types

The target building's properties can impact the magnitude of energy demand changes from the microclimate since the cooling coil usage also depends on the internal loads and size of the building. Several models of varying sizes, passive solar gains and internal loads have been created to cover a more extensive variety of target buildings. The properties of the three buildings/rooms are summarized in Table 5.2.

Table 5.2: Summary of target room properties.

Models	**Size (m^2)**	**Glass to floor ratio (%)**	**Number of occupants**	**ΔT variance**
Small office	30	15	4	0-3.5; increments of 0.5
Medium office	60	13	10	0-3.5; increments of 0.5
Large office	160	43	20	0-3.5; increments of 0.5

5.3 Model Validation

The source room is modeled for each target room to have temperature difference variations covering the spectrum of what was measured during the measurement campaign. This is done at 0.5°C increments. Next to the average ΔT, other microclimate characteristics must also be validated across the simulation period. Firstly, the peak temperature difference should match the measurements to receive an accurate estimation of the peak load for the cooling coil. These peaks should also occur in a somewhat similar frequency as during the measurements, and the general pattern between wind speed, solar irradiation and temperature difference should match. For this, the three parameters are plotted as a heat map as shown in Figure 5.1.

Figure 5.1: General relation between solar irradiation, wind speed and the resulting ΔT of Ch. 1 - Ch. 8 (5 cm measurement - 200 cm) and the BSim simulation results. Simulation data on the left, Measured weather data on the right. The data represent hourly averages values.

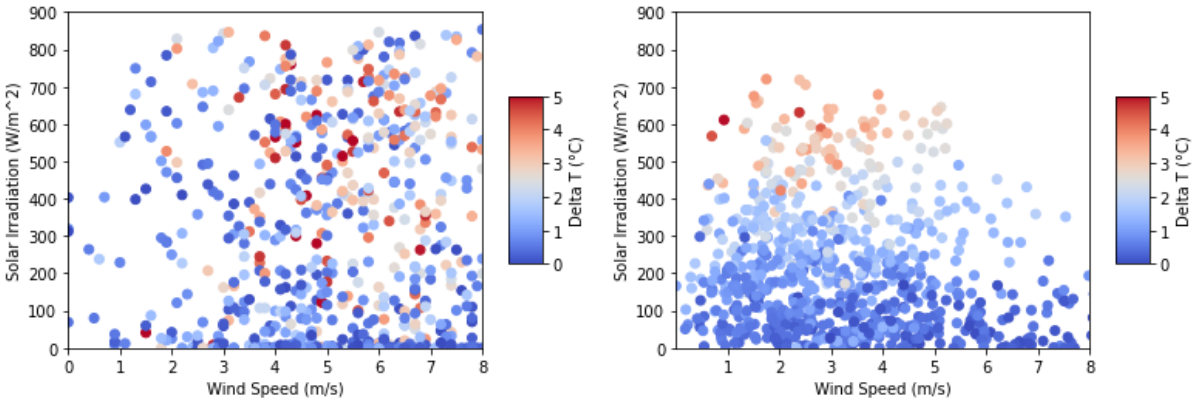

The scale of peak temperature differences and the position thereof on the heatmap somewhat match, meaning that the simulation results are an acceptable representation of the microclimate. The wind speed in the DRY2010 weather file is generally higher than the measurement results, making a perfect match impossible.

5.4 Simulation results

Running the simulations for three office types explained in Table 5.2 indicates the general magnitude of temperature difference impacts on the efficiency of cooling coils. As shown in Figure 5.2, the impact increases almost linearly with increasing ΔT values.

Figure 5.2: Graphical representation of conversion table from ΔT to increase in annual and peak energy demand of cooling coils for offices of three different sized. Shaded areas indicating ΔT from measurement results for daytime average (green) and peak 5% (blue) .

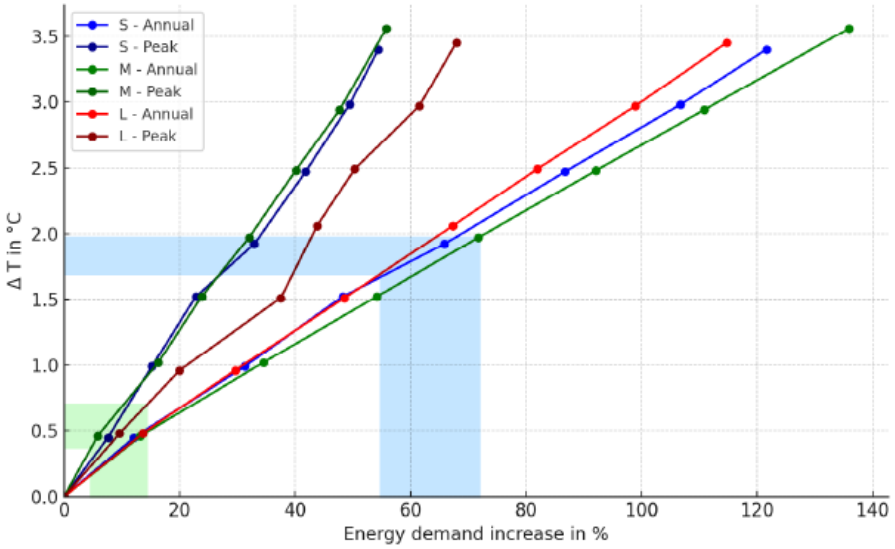

The trend is very similar between the different offices, with the annual energy demand being impacted more than the peak loads. Yet, both show significant increases in the energy demand. Looking at the key ΔTs from Figure 3.6, the daytime ΔT range between 30 and 50 cm above the roof would result in an average increase of the annual energy demand for cooling between 10% and 15% depending on the building size and internal loads. The peak 5% of the recorded ΔTs for these channels lays between 1.65°C and 2°C resulting in an increased peak load capacity between 55% and 73%, meaning that ideally, the cooling coil needs to be dimensioned significantly larger compared to scenarios without a microclimate related temperature increase.

5.5 Microclimate mitigation strategies

The results shown in Chapter 5.4 indicate a significant impact on the energy demand of cooling coils caused by temperature stratification in the microclimate. If engineers judge this negatively impacts their designs, the effect can be mitigated in several ways. Chapter 3 determines the solar irradiation to be the driving factor for increased temperatures in the microclimate, so positioning a roof-mounted HVAC unit in a shaded place on the roof would be the first and most impactful step. Alternatively, additional structures providing shade on the inlet area can be implemented, or the unit can be positioned so that the body of the unit shields the inlet area from direct solar irradiation, f.e. with a north-facing inlet duct. Secondly, the inlet height of the ventilation unit plays a significant role in the temperature increase, so this is a variable that engineers can adjust. Either the inlet duct can be placed as high as possible above the roof surface, ideally between 100 cm and 200 cm, where the smallest ΔTs are found according to Figure 4.2, or if a standardized AHU is used where the inlet height is not adjustable, the unit has

a whole can be raised, subsequently raising the inlet height. Lastly, wind exposure can be used to reduce the temperature of the microclimate zone in which the AHU is positioned. The natural air exchange of the wind can be utilized by purposefully placing the unit in a section of the roof where the predominant wind direction is the least obstructed.

Chapter 6

Discussion

The magnitude of temperature stratification within the vertical 2-meter microclimate zone on flat roofs has been successfully determined, and the impact of the most significant environmental parameters (solar irradiation and wind speed) within the microclimate have been numerically quantified. Additionally, the potential effect of the microclimate temperature stratification on the efficiency of cooling coils for a selection of case buildings has been determined. The relationships between environmental variables and the resulting temperature difference have been modeled, and a prediction tool has been created to apply this research's findings to third-party roofs. This improves the ability of engineers and architects to judge the benefits and drawbacks of different ventilation unit designs and placements when these are located within the microclimate. While general guidance for microclimate impacts on ventilation units is provided, this research has not accounted for many minor environmental variables and building characteristics that also influence the microclimate. The relationship between solar irradiation and temperature stratification can accurately be predicted, giving engineers important insights, but in the current state of the prediction tool, there is no possibility of including the impact of partial shade from surrounding structures on the ventilation unit, severely limiting the application range of the models. With wind being an essential factor influencing the microclimate, the degree of shielding plays an equally significant part, but to include this in the analysis, case-specific information on peripheral structures on a roof and the exact wind direction need to be known. The analysis and prediction tool currently neglect this. Further, the measurements have only covered dark bitumen roofs, meaning that the analysis results and prediction tool only apply to roofs with the same albedo. To address this, further measurements on roofs with different building materials are needed, which would allow the inclusion of the surface's albedo as a variable in the analysis. The measurements and prediction tool only cover summer climates and point out negative impacts on the cooling coil of ventilation units. Potential benefits for periods where the ambient temperature falls below the ventilation inlet temperature set point are not investigated. Yet, they are necessary for a nuanced judgment of the year-round impact of the microclimate since temperature increases during wintertime may offset parts of the energy demand increase in the summer. In conclusion, the current state of the analysis and prediction tool provides a thorough understanding of the microclimate during the summer period, giving engineers and architects a foundation for incorporating microclimate impacts into their designs. Still, several improvements must be made to expand the cases where the results and findings can be applied to other buildings.

6.1 Suggestions for future work

Further measurements and development of the prediction tools are needed to resolve the shortcomings outlined in the discussion. While the measurement campaign of this project has been more extensive than any other research on the field of microclimate, it failed to capture the microclimate across a full calendar year, resulting in only partial data points for the winter month. To remedy this and to be able to extrapolate findings for the heating period as well, measurements should be expanded to cover an entire year. Further, the weather stations have been equipped with 8 temperature sensors for different heights above the roof, but only one anemometer placed at 200 cm above the ground. Due to this, a discrepancy between the actual wind speed experienced by each channel individually and the measured windspeed may have introduced an error, reducing the accuracy of the determined regression between wind speed and microclimate temperatures. Having an independent anemometer per temperature sensor can avoid this error. Regarding the prediction tool, many shortcomings regarding its versatility have been outlined in the discussion. The most direct solution for this would be creating a white box model that incorporates all thermodynamic principles at play in the microclimate, which is then validated with the measured

data. To improve the existing black box model, more data and more environmental variables would improve the accuracy and bring its accuracy and versatility closer to a white box model. Specifically, environmental parameters that impact the heat transfer within the microclimate, like relative humidity, , a windshield coefficient, the wind direction and measurement data from roofs with different albedos, would improve the model's versatility. Currently, the energy demand analysis has been solely based on simulations of the microclimate and cooling coil efficiencies. Complementing this step with empirical Building Management System (BMS) data from an actual AHU in the microclimate would allow for a more thorough model validation.

Chapter 7

Conclusion

Aligning with previous research on the topic, the micro-climate on roofs has been found to significantly differ from the general climate typically used in building design and energy calculations. A persistent temperature stratification has been identified, together with the primary environmental factors of solar irradiation and wind speed affecting it. As part of this research, this phenomenon has been found to impact the energy demand of cooling coils, revealing a substantial discrepancy between the assumptions made during ventilation design and the actual conditions that HVAC units are exposed to when positioned within the microclimate. The measurements of temperature, solar irradiation, and wind speed have been used to model the interplay between these variables in the microclimate, and the resulting models now enable engineers to attain a better understanding of the thermodynamic implications of placing a ventilation unit on the roof. The microclimate models used in the prediction tool allow engineers to transfer the results from this study to other roofs, aiding in calculations and the decision-making for ventilation design. While there are limitations in the tool's versatility to deal with conditions significantly different from the measurements, it still indicates general trends of how the microclimate differs from the local climate. Once the shortcomings of the prediction tool are resolved with further measurements and a more complex model that includes more environmental variables, it has the potential to increase the accuracy of energy models of buildings and prevent under-dimensioning of cooling coils, as well as indicate the most efficient and sustainable placement of HVAC units. This study enhances the precision of microclimate modeling on urban rooftops, offering a more accurate framework for HVAC system design and energy efficiency, thereby contributing to advancing urban building practices in response to environmental variables.

Bibliography

[1] Tianzhen Hong, Yujie Xu, Kaiyu Sun, Wanni Zhang, Xuan Luo, and Barry Hooper. Urban microclimate and its impact on building performance: A case study of san francisco. *Urban Climate*, 38:100871, 2021.

[2] Hicham Johra and Mathilde Lenoël. Micro-climate measurement campaign of the outdoor air temperature around an office building in denmark during the summer 2022, Apr 2023.

[3] Karl Grau Sørensen Kim Bjarne Wittchen, Kjeld Johnsen. Bsim: Building simulation. Technical report, Aalborg University, 2007.

[4] Martín Mosteiro-Romero, Daniela Maiullari, Marjolein Pijpers-van Esch, and Arno Schlueter. An integrated microclimate-energy demand simulation method for the assessment of urban districts. *Frontiers in Built Environment*, 6, 2020.

[5] Kristian Pagh Nielsen. Dmi report 18-20 2001 - 2010 danish design reference year. update and supplementary datasets., 2019.

[6] Krunoslav Premec. Cimo guide preliminary 2018 edition, 2018.

[7] Martin Veit and Hicham Johra. How to use arduino uno for low-cost temperature measurements with pt 100 sensors. DCE Lecture Notes 80, Aalborg University, Department of the Built Environment, Aalborg, Denmark, November 2022. Accessed: December 20, 2023.

[8] Videncenter for Energibesparelser i Bygninger. Energikravene i BR18: En kvikguide til byggefagfolk om Bygningsreglementet, September 2022. Revised Edition.

[9] Peter Grunnet Wang, Mikael Scharling, Kristian Pagh Nielsen, Kim Bjarne Wittchen, and Claus Kern-Hansen. 2001 – 2010 danish design reference year: Reference climate dataset for technical dimensioning in building, construction and other sectors. Technical Report 13-19, Copenhagen, 2013.

[10] WeatherSpark. Average weather in aalborg denmark year round. `https://weatherspark.com/y/65478/Average-Weather-in-Aalborg-Denmark-Year-Round#Figures-WindDirection`, 2024. Accessed: [06.01.2024].

Appendix A

Appendix - Weather Station

Appendix A provides a detailed description of the weather stations used for the measurement campaign.

A picture of the weather station employed on the roof of PON can be seen in Figure H.3 with the main components highlighted. The main features of the weather station are the central wooden structure, which holds everything in place; the sensors, which are placed around the main frame; as well as all the electronics, which are placed inside the weatherproof electrical box with a microcontroller steering the sensors and logging the data.

Figure A.1: Photo of a weather station on the roof of case building (PON). Main components labeled.

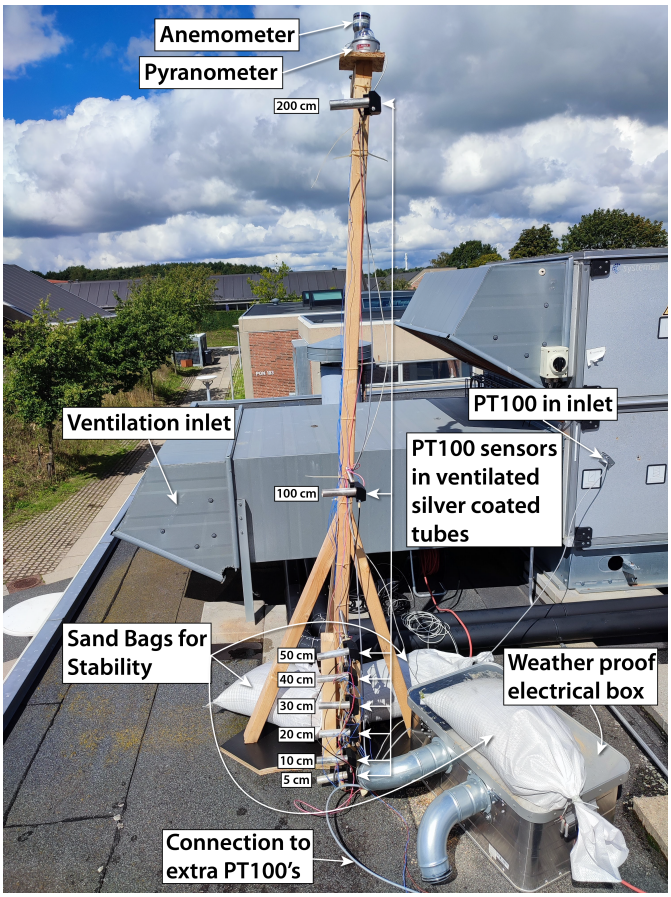

In the following sections, the main characteristics of the components, as well as significant changes to the original design, will be highlighted to allow for the reproduction of the measurements.

A.1 Main Structure

The microclimate weather station's initial design heavily relied on steel components as the central column, clamps, and footing. Considering the exposure to rainy weather during the measurement period, the main structure would have rusted heavily and destroyed the components. To prevent this, wood has been chosen as the material for the structural elements. A 2050 mm long 45 x 45 mm central column functions as the attachment point for the sensors. The column has been braced with 5 diagonally attached beams which have been screwed into the column and the 600 mm x 600 mm footplate. The corner underneath the ventilated tubes with the PT100 sensors has been removed to have the actual roof material right underneath the sensors, as shown in Figure A.2. The top surface of the wooden footplate has been chosen to resemble the color of the bitumen roof, which can be found on both measurement locations.

Figure A.2: Close up of sawed footplate.

To further support the main structure, the footplate has been supported with two 30 kg sandbags. The ventilated tubes have been attached to a threaded rod led through a threaded hole drilled into the main wooden column. The main column further acted as a support for all the wiring that went along the weather station.

A.2 Sensors

The weather stations included three different kinds of sensors covering temperature sensors at different heights above the roof, wind speed and direction measurements from an anemometer, and solar irradiation measurements from a pyranometer.

A.2.1 Temperature sensors

The project's main objective is to receive detailed temperature readings from various heights above a roof surface. The main criteria for the temperature sensors are that they can reliably provide temperature data for the intended temperature range at high sample rates, despite exposure to adverse weather conditions in an outdoor setting. For this purpose, PT100 resistance thermometers have been chosen, which are soldered onto a 4-wire cable and connected to an Adafruit MAX31865 amplifier to be read by the Arduino microcontroller. The following assembly guide for the PT100 soldering has been followed: [7].

For each weather station, a total of 11 sensors have been connected. The original intended use was eight sensors for the main rig measuring the temperature stratification, two sensors for a small rig placed ˜10 meters away from the main weather station structure, and an 11^{th} sensor for placement inside an AHU if present in the vicinity of the weather station. An AHU was only present for PON. Due to hardware failures of multiple PT100s and the lack of necessity to record on additional places on the roof, faulty sensors have only been replaced for the main measurement column, resulting in 8 (TMV) and 9 (PON) working sensors, respectively. The sample rate for all temperature sensors has been set to a four-second interval to achieve a level of detail that allows investigations into short-term fluctuations of the microclimate. For PON, the 9^{th} sensor has been placed inside the inlet of the nearby ventilation unit.

Direct solar irradiation protection and ventilation

To prevent direct solar irradiation on the resistance thermometers from distorting the readings, the sensors have been placed centrally inside a silver-coated metal tube of ˜12 centimeters in length with a diameter of 2 centimeters. The silver coating has been polished prior to installation. To prevent the tube and equipment close to the sensor from distorting the measurement, the tube has also been ventilated with small electrical fans continuously blowing a gentle air stream through the tube. The chosen fan is an ebmpapst 255N with a nominal voltage of 5V and an RPM of 9600. The fan has been positioned in a way to blow into the tube. All fan's power supplies have been soldered together in parallel.

A.2.2 Wind and solar irradiation measurements

Anemometers and pyranometers have been attached to the main structure of the weather stations to gain site-specific wind speed and solar irradiance measurements. These have been attached to the upper tip of the wooden center pole at a height of ˜210 centimeters. The pyranometer has been positioned so that at no point in the sun's path is a shadow from the structure itself being cast onto the detector surface. The anemometer has been positioned so that the form of the weather station does not obstruct the wind.

The anemometer has been connected to the microcontroller, storing its output on the integrated SD card, and measures at the same interval as the PT100s. The pyranometer has been linked to a separate data logger and set to an interval of minutely data readings.

A.3 Micro controller

A separate microcontroller controls each weather station. An Arduino Mega 2560 has been chosen due to the many available digital pins. The microcontrollers have been extended with a set of 2 breadboards, which provide additional pins for daisy-chaining the SPI communication pins of several PT100s and their amplifiers in series. Only the CS pin of each amplifier has been wired individually to a digital pin on the microcontroller. Further, each microcontroller has been equipped with an RTC clock module to record the precise timing of each measurement interval. An anemometer has been connected to the analog pins on the microcontroller. Lastly, an SD-card module was linked to each microcontroller to log all the recorded data, where each data point was written into a .csv text file.

Summary of microcontroller components:

A.4 Rain protection

To ensure the setup functions during any weather condition, several steps have been taken to make the setup rain-resistant. The electrical fans attached to the ventilated tubes have been enclosed in a 3D-printed housing. The housing has been equipped with a diagonally downwards-facing shaft so as not to disturb the airflow. For a drawing of the fan casing, see Figure A.3.

Table A.1: Microcontroller components

Function	Component	Item name
Microcontroller	Arduino Mega 2560	Computer to steer all sensors and log data
Breadboard	830 pin Arduino Breadboard	Pin extension board for microcontroller. Allows serial connection of amplifier SPI communication pins
Jumper cable	Male-Male & Male-Female (for SD card reader) 10 - 20 cm jumper cable	Power supply and data connection for components
Amplifier	Adafruit MAX 31865	Allows reading of low resistance thermometers
Resistance Thermometer	PT100	100 Ohm platinum resistance thermometer
Clock	DS3231 Real Time Clock Module	logging of date and time data
SD card reader	Micro SD TF Card Shield Module	Interface for SD card
SD card	SanDisk 16gb micro SD card	stores logged data. Must be non-XC, FAT32 formatted SD card.
Anemometer	—	—

Figure A.3: Sketch of 3D printed fan casing.

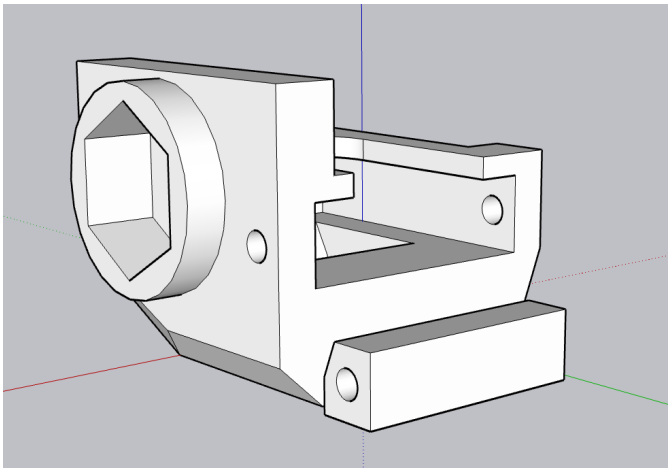

The fan casing additionally functioned as the anchoring point of the PT100s, tube, and fan onto the main rig by having a hexagonal mold in which a nut was glued, which was then screwed onto a threaded rod extending from the central column. Further, a rainproof ventilated electrical box has been added to the setup in which the power supply and electronics have been stored. One electrical box opening is a cable outlet, while the other hole is a ventilation slot.

Figure A.4: Photo of the contents of the electrical box positioned at PON.

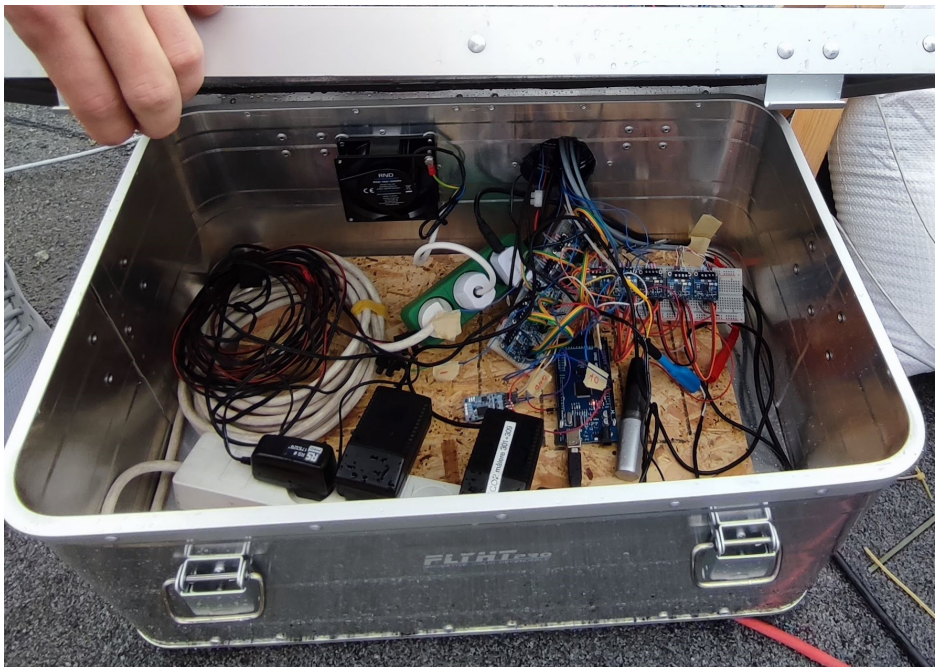

The electrical box housed the following components:

- Extension cables
- Power Supplies
  - Fans of primary weather station
  - Fans of secondary weather station
  - Electrical box fan
  - Anemometer
  - Pyranometer
  - Arduino Mega 2560
- Arduino Mega 2560 + 2 Bread Boards
- Amplifiers for PT100's
- Data Logger for Pyranometer
- Amplifier for Pyranometer

The Arduino setup was fixed on a timber baseplate inside the electrical box to prevent the jumper cables from ripping out of the pins, thus making it more stable when it was transported. The box has been supported with a 30kg sandbag to ensure it doesn't move in the wind.

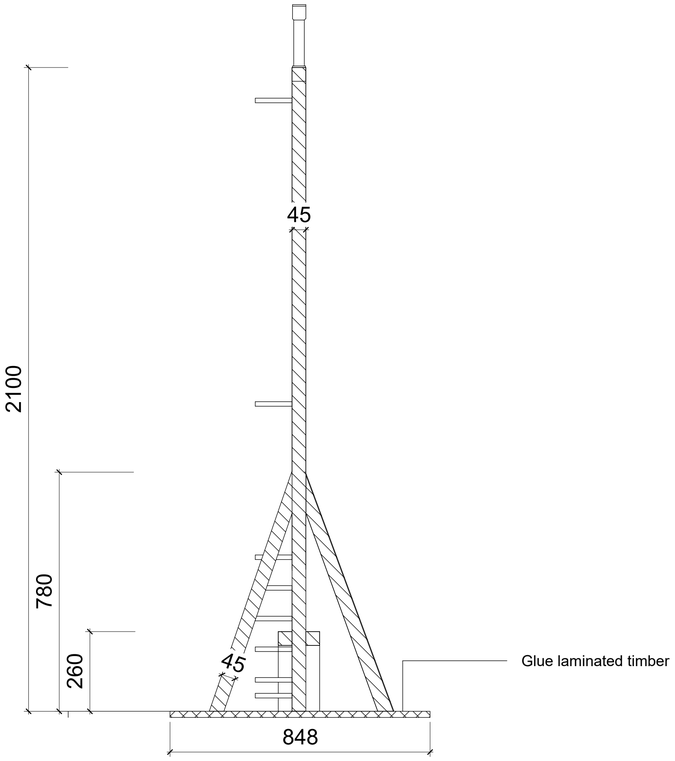

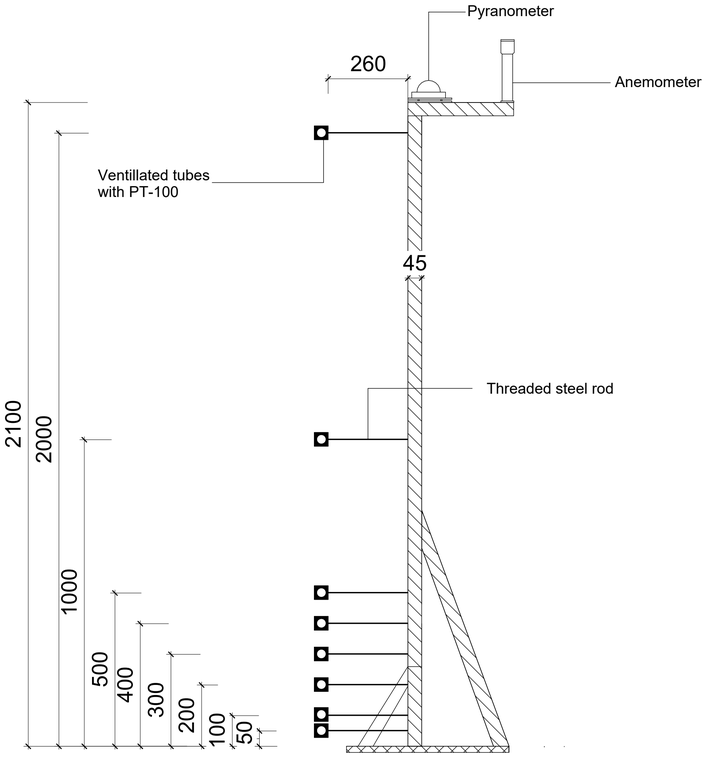

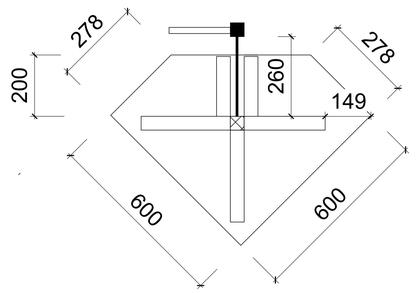

Timber stud, 45x45mm

Glue laminated timber (baseplate)

Rev	Description	Date

CODE	SUITABILITY DESCRIPTION
STATUS	PURPOSE OF ISSUE

AUTODESK
www.autodesk.com/revit

PROJECT
Master thesis

TITLE
Weather station

CLIENT
AAU

DRAWN BY	CHECKED BY	DATE
Author	Checker	01/05/24

SCALE (@ A1)	PROJECT NUMBER
1 : 10	Project Number

DRAWING NUMBER	REV
A101	

08/01/2024 17:02:51

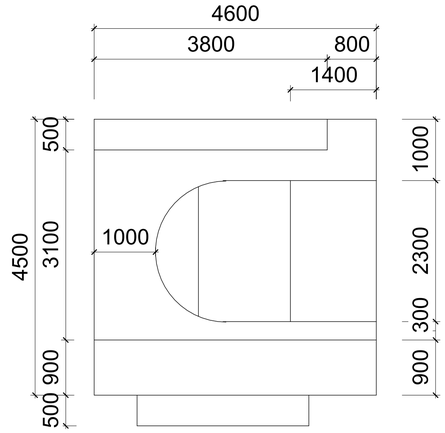

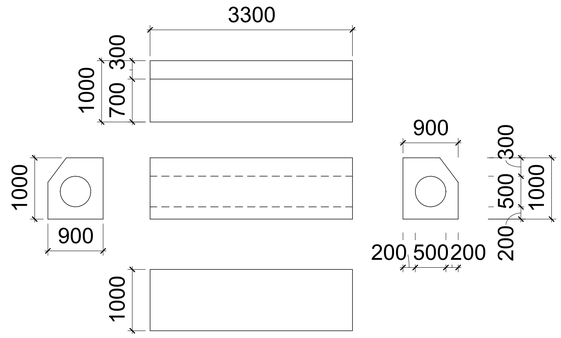

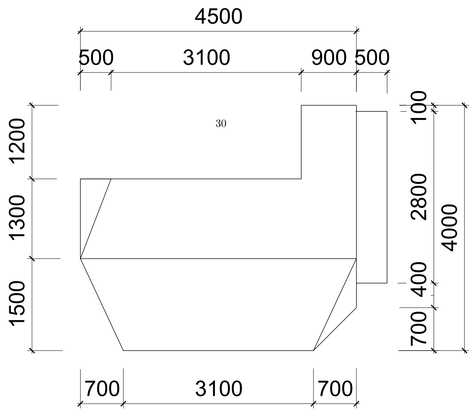

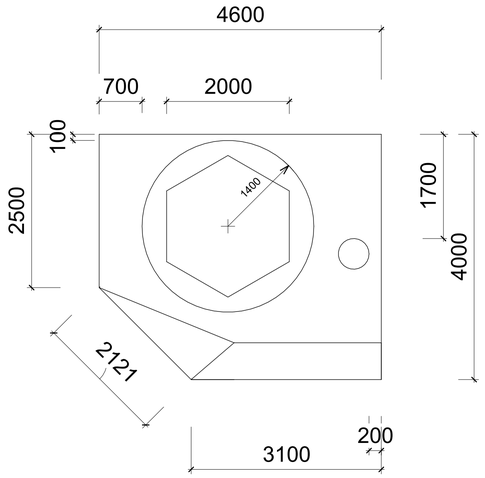

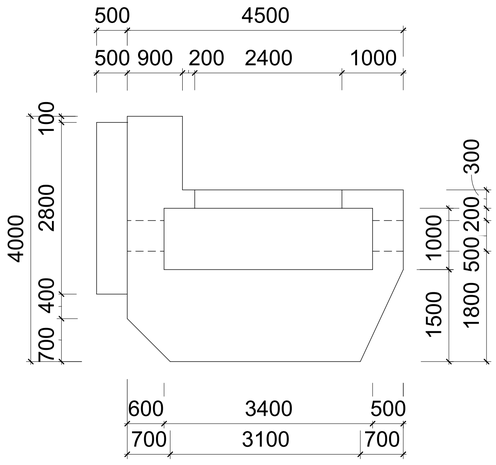

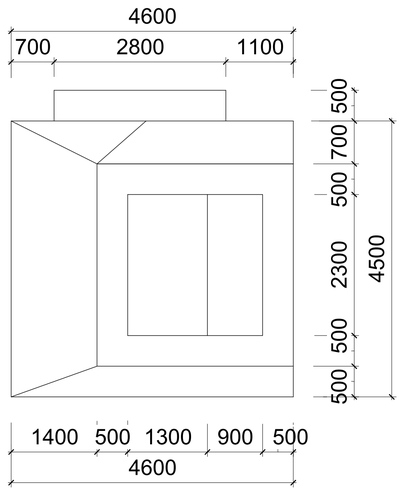

Rev	Description	Date

CODE	SUITABILITY DESCRIPTION
STATUS	PURPOSE OF ISSUE

AUTODESK
www.autodesk.com/revit

PROJECT
Master thesis

TITLE
3D printed clamp

CLIENT
AAU

DRAWN BY	CHECKED BY	DATE
Author	Checker	01/23/07

SCALE (@ A1)	PROJECT NUMBER
1 : 50	Project Number

DRAWING NUMBER	REV
A100	

08/01/2024 18:20:16

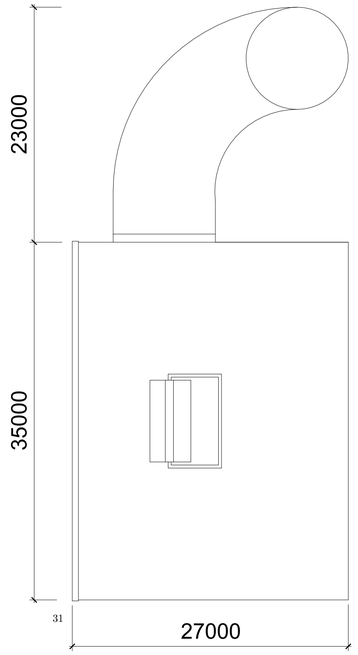

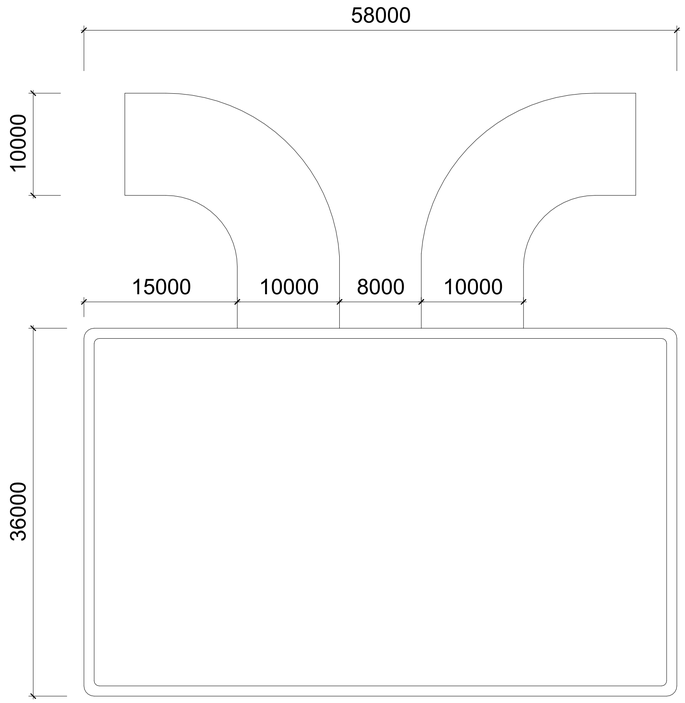

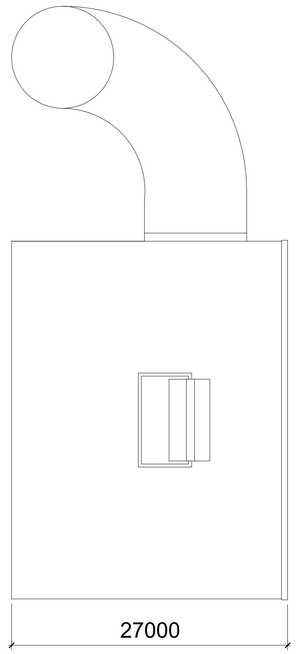

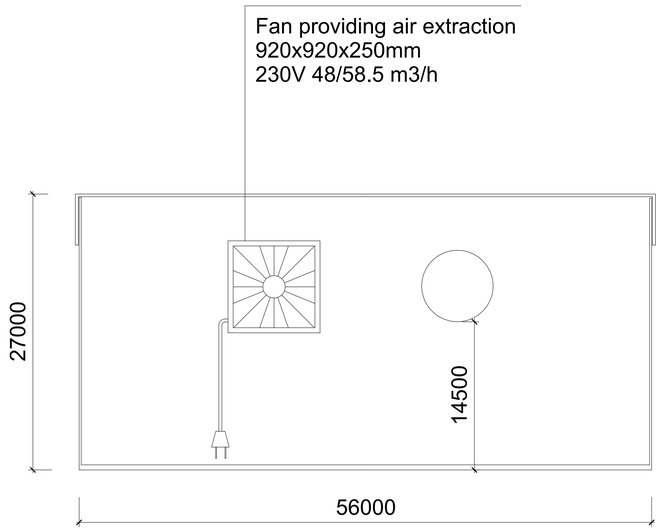

Rev	Description	Date

CODE	SUITABILITY DESCRIPTION
STATUS	PURPOSE OF ISSUE

AUTODESK
www.autodesk.com/revit

PROJECT
Master thesis

TITLE
Ventillated box

CLIENT
AAU

DRAWN BY	CHECKED BY	DATE
Author	Checker	01/05/24

SCALE (@ A1)	PROJECT NUMBER
1 : 300	Project Number

DRAWING NUMBER	REV
A103	

08/01/2024 19:38:49

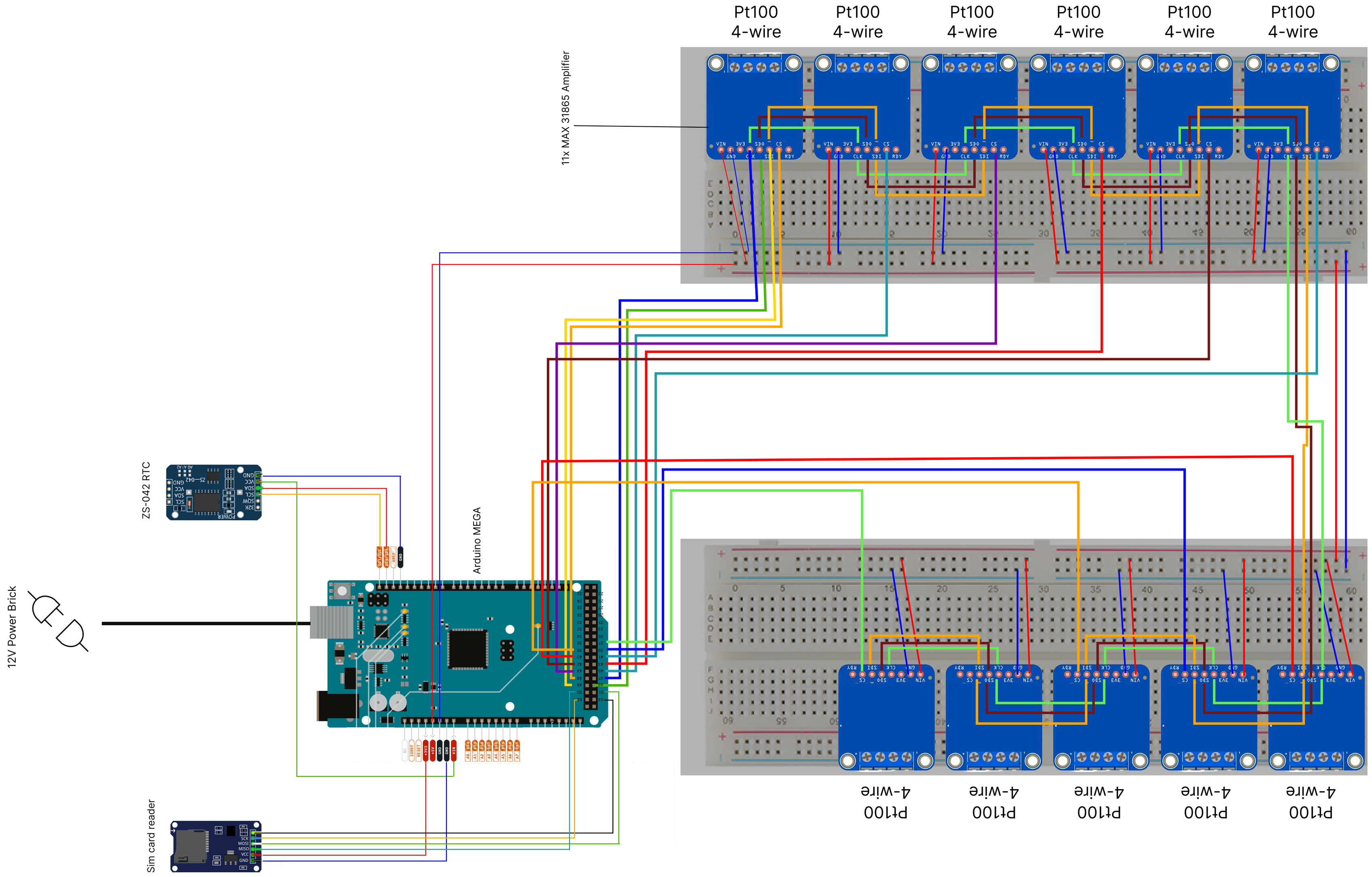
Pt100
4-wire
Pt100
4-wire
Pt100
4-wire
Pt100
4-wire
Pt100
4-wire
Pt100
4-wire
11x MAX 31865 Amplifier
ZS-042 RTC
Arduino MEGA
12V Power Brick
Sim card reader
Pt100
4-wire
Pt100
4-wire
Pt100
4-wire
Pt100
4-wire
Pt100
4-wire

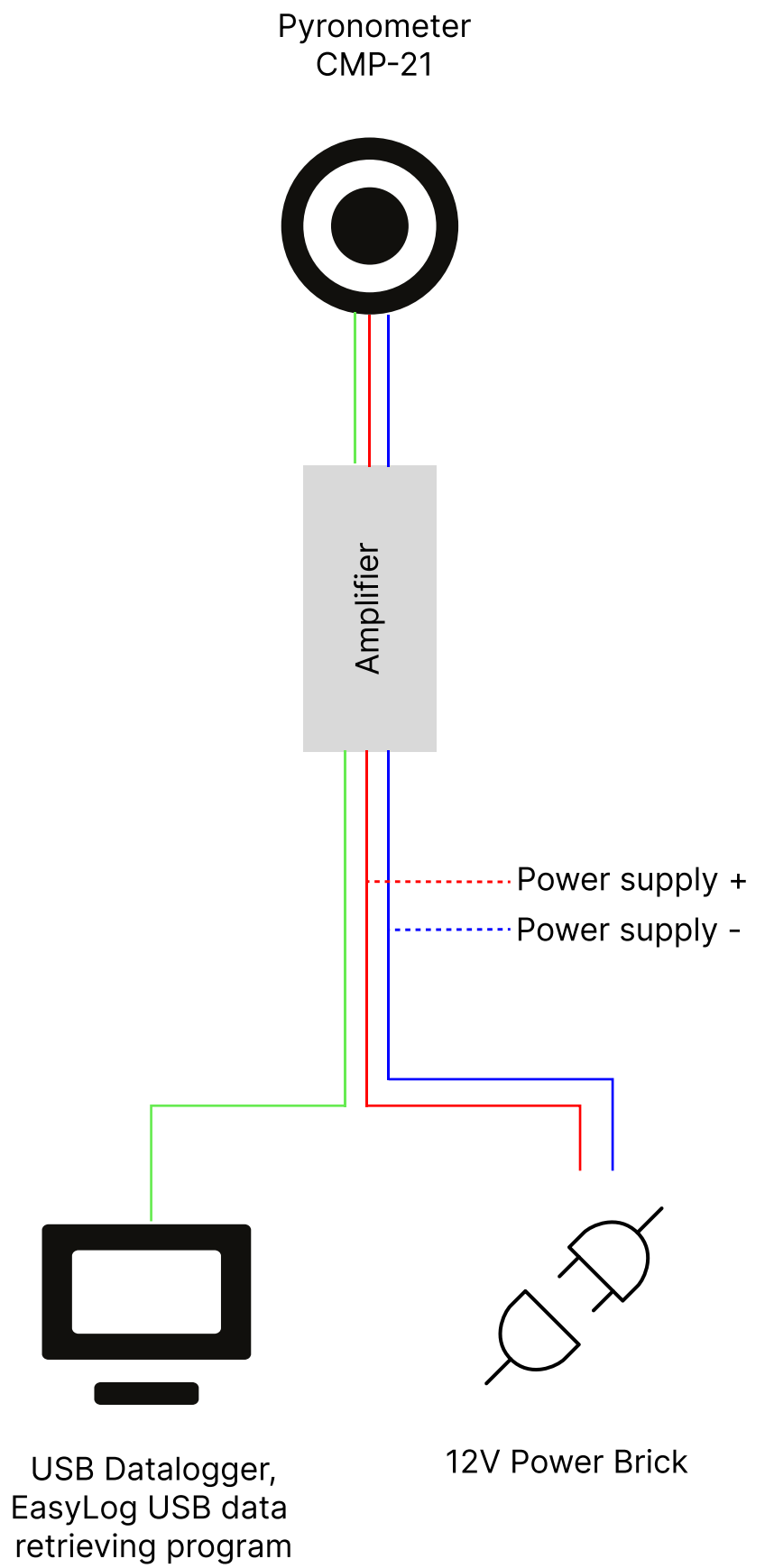
Pyronometer
CMP-21
Amplifier
Power supply +
Power supply -
USB Datalogger,
EasyLog USB data
retrieving program
12V Power Brick

Appendix B

Appendix - Measurement Period

This appendix contains a detailed description of the measurement campaign process, covering the chosen locations and time frames of when what was measured.

B.1 Measurement locations

A total of four weather stations have been constructed, which were intended to be used on a variety of roofs, primarily covering different roofing materials and roofs with different environmental exposures to sun and wind. Gaining access to roofs, which the university does not administer, turned out to be challenging, however, leading to the geographical boundary being the university campus. Two roofs with strongly opposing properties regarding the building height and wind exposure have been chosen from the available campus roofs. Roofs with different solar shading or different roofing materials were not available. The two chosen locations are indicated on the map in Figure B.1.

Figure B.1: Location of roofs where weather stations have been placed. MapsIndoors. (2024). AAU Campus Map. Retrieved from https://clients.mapsindoors.com/aau/57482221bc1f570e288b8ef0/search?cat=library

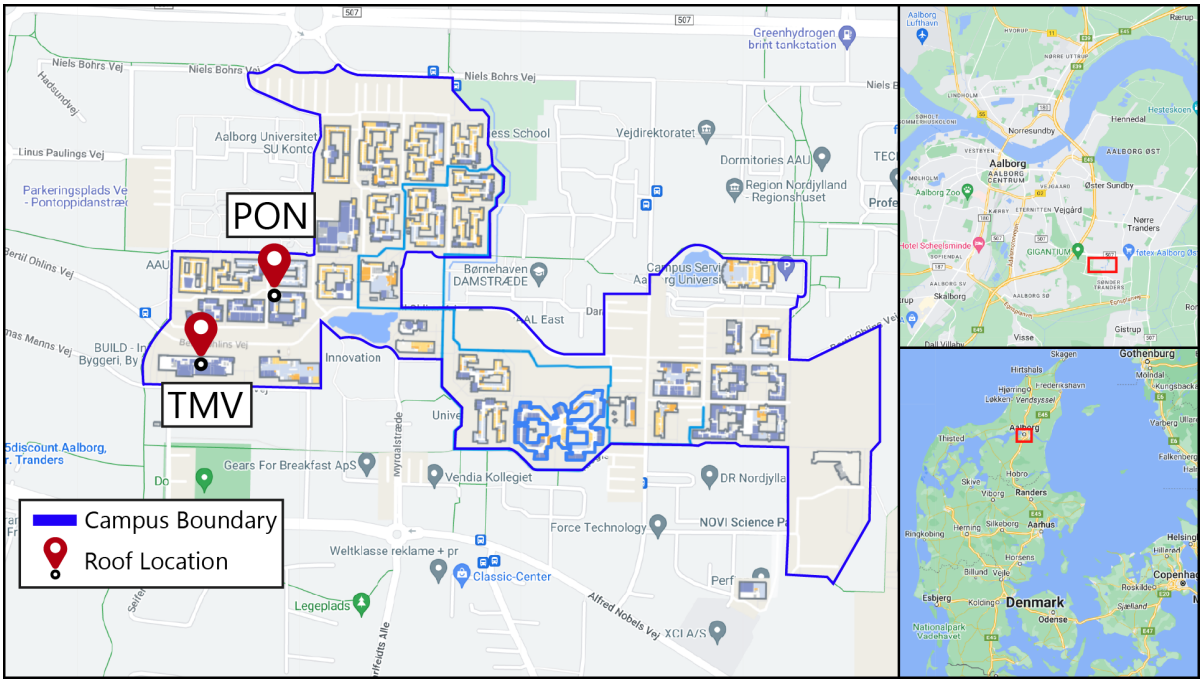

Both locations are located in Aalborg which is exposed to predominantly western winds as shown in Figure B.2.

Figure B.2: Preminant wind direction in Aalborg. Source: [10]

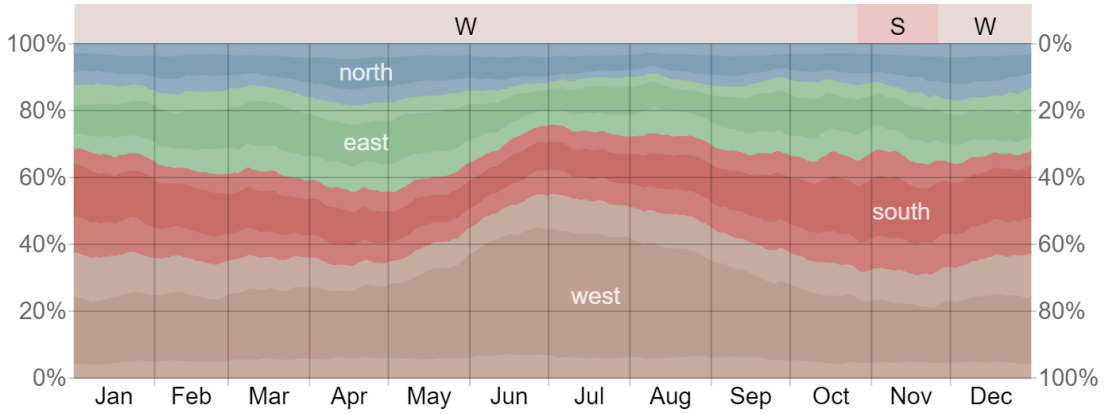

B.1.1 Location 1: TMV

TMV is a roughly 17m tall building with a large flat roof. There are several structures on the roof, such as skylight extrusions, a cased-in ventilation unit, a raised gangway with experiment setups, an additional story with a small laboratory, and two staircases extruding the building envelope. It is the tallest building for hundreds of meters around it, and one-half of the roof is entirely void of structures, making it very exposed to the wind. Topographically, shallow hills are scattered around the site, but not enough to impact the wind speed significantly. The location of the weather station on the roof has been chosen to be within the half which is expected to have the highest wind exposure. The weather station has been placed approximately 2.5 away from the edge of the roof, with the temperature sensors extending southwards from the central column. This means the ventilated tubes have an east-west orientation, with the fan blowing air westwards.

B.1.2 Location 2: PON

PON is a 1-story building with a higher than average ceiling height, resulting in a roughly 4.5 meter heigh roof level. The building is surrounded by several buildings of the same and taller heights. The roof has features like a mid-sized AHU, ledges, and long raised skylight extrusion. Here, the weather station has been positioned approximately 70 cm away from the AHU towards the southern side. The sensors are again orientated towards the south, with the ventilated tubes facing in the same direction as on TMV. Due to the density and proximity of roof structures and several buildings of equal or taller height, PON is generally more wind-shielded.

B.2 Overview of sensor up-time

The measurement campaign across the two roofs has been undertaken for 142 days between July 11th, 2023, and November 28th, 2023. During this period, several faults occurred, which have caused missing measurement data across most channels. The Gantt chart in B.3 indicates the availability for all channels used during the measurement campaign, where black indicates continuous measurements and gaps indicate sensor downtime.

Figure B.3: Gantt chart indicating the up-time of sensors from both weather stations used during the measurement campaign. The upper half shows availability channels from PON, while the lower half shows availability from TMV.

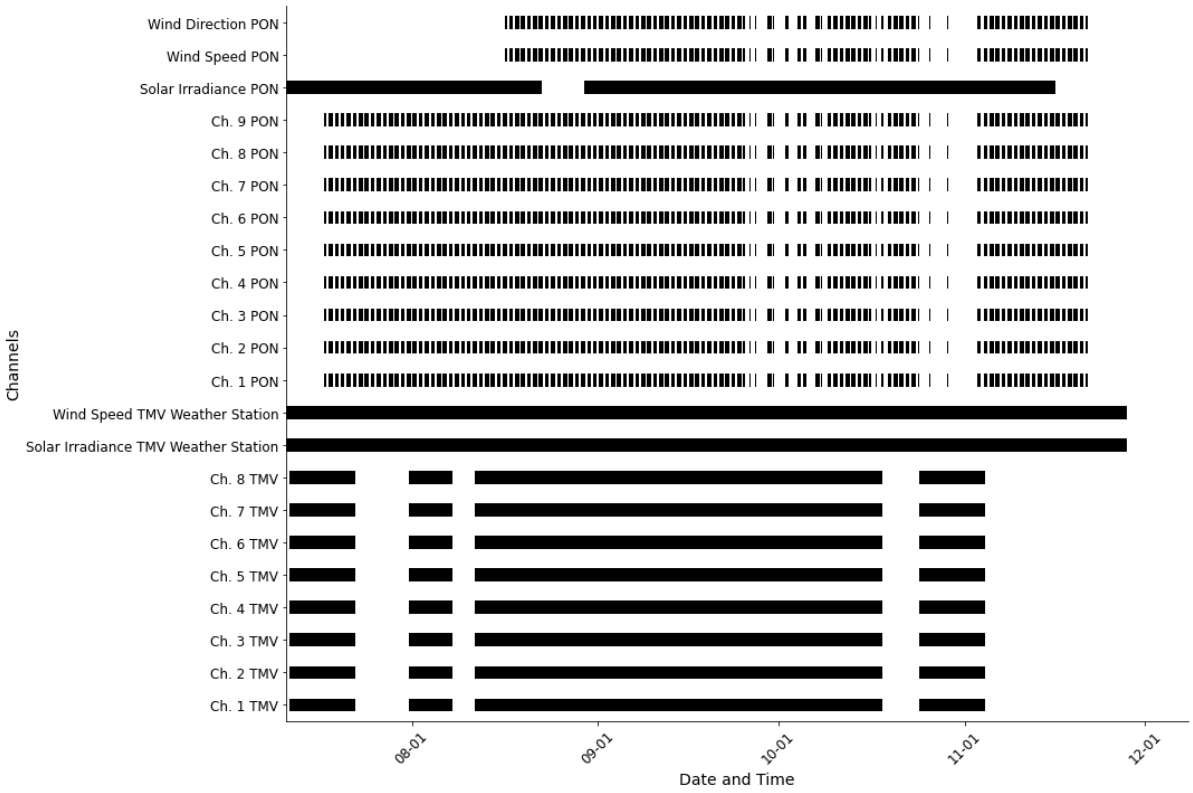

The patchy recordings of PON measurements can be drawn back to the main power supply of the electrical box in which all electronics and controllers were stored, being connected to a plug that shuts off during the night time between 21:00 and 04:00. No other plug was available at the measurement location. The solar irradiance measurements were uninterrupted since the pyranometer was connected to an external data logger with an internal battery to bridge the time without a power supply. Longer gaps in the measurement data can be drawn back to hardware or software failures caused by various reasons from adverse weather or general power outages.

Appendix C

Appendix - Measurement Results

In this chapter, further information on the measurement results are presented.

C.1 Temperature sensor calibration

All temperature sensors used during the project have been calibrated with a temperature sink against a precision thermometer. In the table below, the temperature difference between the precision thermometer and the PT100 readings is presented with the mean error indicated.

Arduino mega, board 1

Sink setting	Ch. 1	Ch. 2	Ch. 3	Ch. 4	Ch. 5	Ch. 6	Ch. 7	Ch. 8	Average
-15	1.68	1.31	1.08	1.42	1.51	2.05	1.15	1.21	**1.43**
0	0.54	0.50	0.50	0.37	0.84	1.04	0.54	0.47	**0.60**
20	0.20	0.20	0.20	0.37	0.40	0.27	0.17	0.10	**0.24**
40	-0.43	-0.35	-0.76	-0.35	-0.25	-0.73	-0.29	-0.39	**-0.45**
60	-1.40	-0.68	-1.54	-1.13	-0.72	-1.37	-0.51	-0.62	**-0.99**

Arduino mega, board 2

Sink setting	Ch. 1	Ch. 2	Ch. 3	Ch. 4	Ch. 5	Ch. 6	Ch. 7	Ch. 8	Average
-15	1.05	1.65	2.35	0.82	1.58	1.51	0.64	0.78	**1.30**
0	1.05	0.84	1.27	0.51	0.70	0.77	0.30	0.30	**0.72**
20	0.58	0.21	0.28	0.21	0.18	0.11	0.11	0.14	**0.23**
40	-0.39	-0.29	-0.52	-0.56	-0.39	-0.42	-0.18	-0.15	**-0.36**
60	-1.20	-0.62	-0.92	-1.23	-0.75	-0.79	-0.38	-0.31	**-0.77**

Arduino Uno, board 3

Sink setting	Ch. 1	Ch. 2	Ch. 3	Ch. 4	Ch. 5	Ch. 6	Ch. 7	Ch. 8	Average
-15	2.12	1.72	0.62	2.35	1.82	1.18	1.25	0.75	**1.48**
0	1.34	0.84	0.47	1.34	1.31	1.34	0.50	0.37	**0.94**
20	0.42	0.34	0.02	0.57	0.38	0.47	0.17	0.07	**0.30**
40	-0.13	-0.10	-0.20	-0.06	-0.23	-0.20	-0.03	-0.20	**-0.14**
60	-0.76	-0.48	-0.62	-0.52	-0.82	-0.82	-0.23	-0.41	**-0.58**

Arduino Uno, Board 4

Sink setting	Ch. 1	Ch. 2	Ch. 3	Ch. 4	Ch. 5	Ch. 6	Ch. 7	Ch. 8	Average
-15	2.09	1.42	1.88	2.12	1.15	2.12	3.06	1.12	**1.87**
0	1.34	0.87	1.31	1.04	0.97	1.24	0.95	0.64	**1.05**
20	0.37	0.27	0.27	0.23	0.34	0.34	0.33	0.10	**0.28**
40	-0.33	-0.30	-0.23	-0.13	0.01	-0.54	-0.64	-0.33	**-0.31**
60	-0.82	-0.55	-0.79	-0.65	-0.38	-1.20	-1.44	-0.72	**-0.81**

For the expected temperature range of 20°C - 30°C, the mean error across all channels is lowest, and with a range of 0°C - 0.3°C it is negligible.

C.2 Premeasurements

Premeasurements have been undertaken to verify the placement choices for the weather stations with a focus on the general impact of structures like AHUs on roofs to receive a better understanding of the causes and impacts on temperature stratification in microclimates.

C.2.1 Impact of AHU on micro-climate

To better understand the influence of an HVAC unit on the microclimate, a short test was conducted before the main measurement period with two weather stations positioned at different distances from an HVAC unit. As seen in C.1, the weather station close to the unit has experienced higher temperatures and a higher temperature difference between the channels.

Figure C.1: Test measurement of 6 hours, visualizing influence of HVAC unit on measurements. Running average of 20 applied for better readability of plot. Close to unit = Left; Far from unit = Right

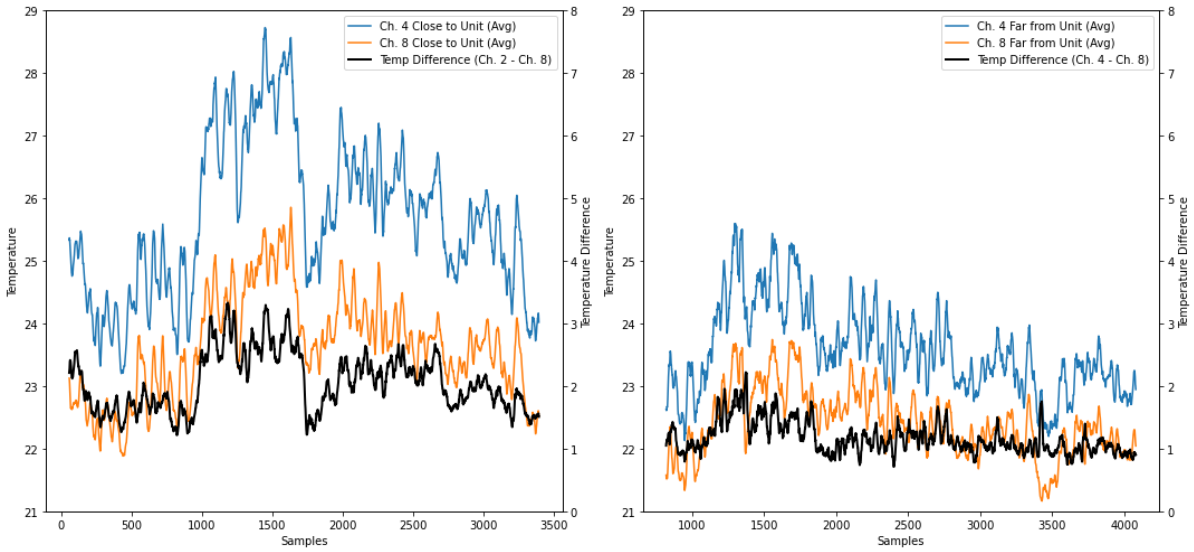

Figure C.2 shows the positioning of the two weather stations.

Figure C.2: Picture of premeasurement setup before wooden weather stations have been constructed.

C.3 General filters applied to raw data

Different measurements have been taken at different sampling rates, requiring the harmonization of the data sets to use them together. Measurements taken with the microcontroller were done in 4-second intervals, while the anemometer and pyranometer from TMV were recorded as minute data from an external weather station. The pyranometer at PON also records at a 1-minute interval since it is connected to an external datalogger, which doesn't support faster sampling speeds. To harmonize the data sets, all data has been averaged to one minute.

As outlined in Appendix B, several hardware and software failures occurred during the 4.5 months of measurements, leading to numerous faulty data points that need to be addressed before meaningful analysis can be done. After manually examining the magnitude of faulty data, the temperature frame of 5°C - 33°C has been chosen as the valid data range. For wind speeds and solar irradiation analysis, daytime values with solar irradiation of <10

have been deemed faulty, and these rows have also been removed. Regarding wind speed, the anemometer at PON has read 0.0 m/s during power supply issues, leading to a filter of >0.1 m/s for all wind data.

C.4 Raw temperature data

Across the measurement period, millions of temperature data points have been collected for both locations. To provide an overview of the general temperature development during the measurement period and the spread between channels, these are shown in Figure C.3.

Figure C.3: Raw temperature data at PON (top) and TMV (bottom) with a 1-day average filter applied

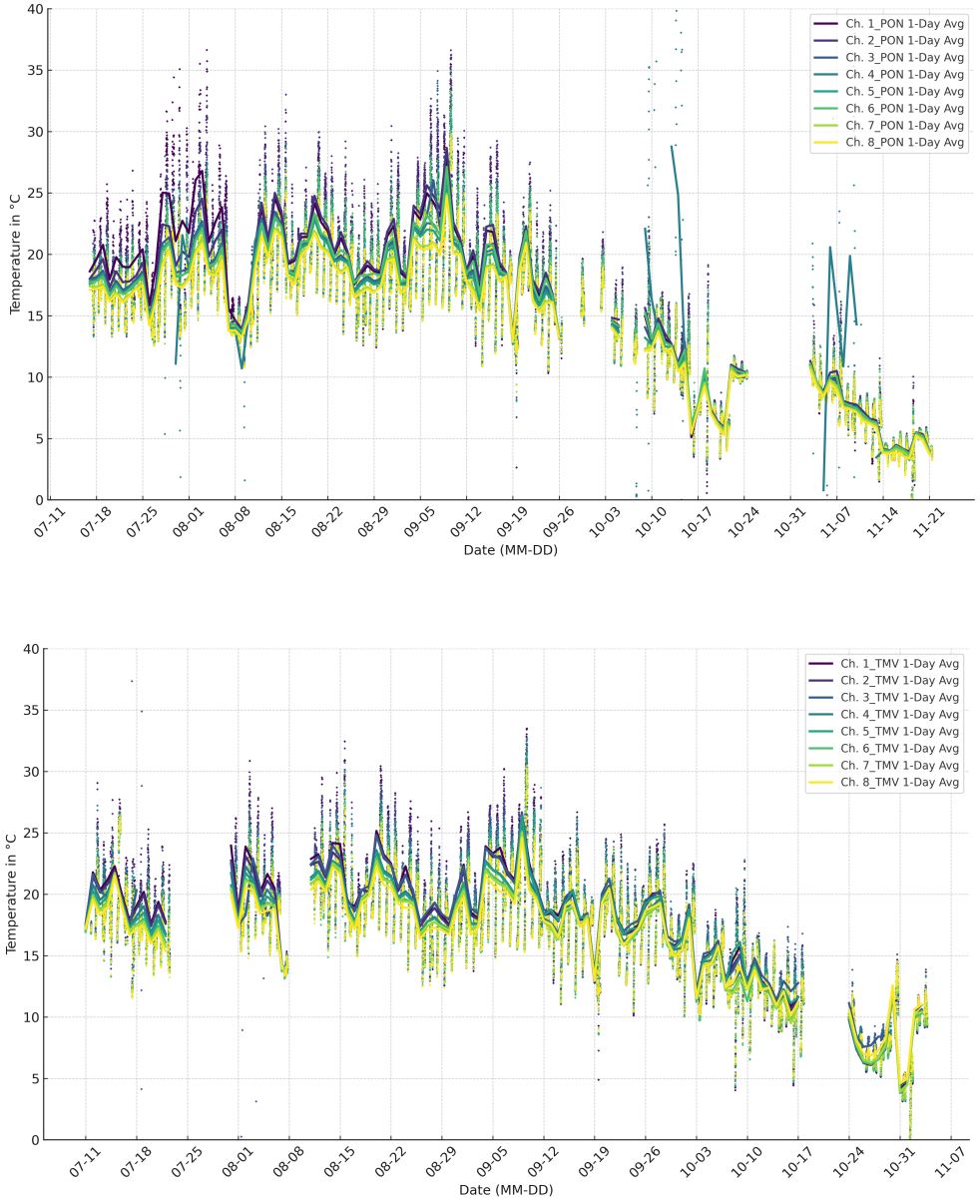

C.5 Weekly ΔT per location for the whole measurement period, daytime and peak 5%

			Week											
Channel	**Height** [cm]	**Criteria**	**29** [°C]	**30** [°C]	**31** [°C]	**32** [°C]	**33** [°C]	**34** [°C]	**35** [°C]	**36** [°C]	**37** [°C]	**38** [°C]	**39** [°C]	**Average** [°C]
Ch. 1	5	Overall	NaN	NaN	0.81	1.09	0.98	1.05	1.03	1.34	0.78	0.64	0.5	**0.91**
		Daytime	NaN	NaN	1.41	1.72	1.55	1.75	1.59	2.27	1.25	0.86	0.75	**1.46**
		Peak 5%	NaN	NaN	2.98	3.76	3.66	3.51	3.54	5.29	4.23	2.71	1.81	**3.50**
Ch. 2	10	Overall	0.56	NaN	1.25	1.08	0.91	0.84	0.73	1.29	0.54	0.27	0.19	**0.77**
		Daytime	1.04	NaN	2.05	1.86	1.7	1.84	1.53	2.53	1.27	0.65	0.59	**1.51**
		Peak 5%	2.77	NaN	4.26	4.31	4.6	4.59	4.11	6.26	4.88	3.16	2.05	**4.10**
Ch. 3	20	Overall	0.35	NaN	0.89	0.72	0.59	0.67	0.58	1.01	0.39	0.26	0.23	**0.57**
		Daytime	0.82	NaN	1.57	1.41	1.13	1.41	1.1	1.91	0.82	0.49	0.52	**1.12**
		Peak 5%	2.55	NaN	3.15	3.65	3.36	3.83	2.84	4.62	2.7	1.99	2.05	**3.07**
Ch. 4	30	Overall	0.09	NaN	0.45	0.4	0.38	0.42	0.38	0.54	0.32	0.23	0.15	**0.34**
		Daytime	0.33	NaN	0.92	0.75	0.7	0.81	0.67	1.05	0.57	0.46	0.4	**0.67**
		Peak 5%	1.5	NaN	2.17	1.99	1.93	2.02	1.73	2.59	2.21	1.99	1.63	**1.98**
Ch. 5	40	Overall	0.19	NaN	0.29	0.25	0.27	0.3	0.32	0.54	0.3	0.11	0.09	**0.27**
		Daytime	0.46	NaN	0.58	0.6	0.57	0.67	0.58	1.07	0.56	0.17	0.14	**0.54**
		Peak 5%	1.52	NaN	1.51	1.87	1.74	1.78	1.54	2.68	2.19	1.07	0.93	**1.68**
Ch. 6	50	Overall	0.02	NaN	0.08	-0.23	0.19	0.16	0.24	0.36	0.14	0.09	-0.06	**0.10**
		Daytime	0.18	NaN	0.29	0.18	0.54	0.51	0.52	0.85	0.33	0.2	-0.05	**0.36**
		Peak 5%	0.84	NaN	0.84	1.23	1.9	1.62	1.84	2.78	2.75	2.05	0.76	**1.66**
Ch. 7	100	Overall	0.14	NaN	0.22	0.14	0.16	0.23	0.26	0.23	0.05	0.07	0.06	**0.16**
		Daytime	0.26	NaN	0.36	0.33	0.28	0.34	0.28	0.34	-0.03	0.01	-0.02	**0.22**
		Peak 5%	0.8	NaN	0.69	0.74	0.69	0.7	0.62	0.78	0.59	0.44	0.39	**0.64**

C.6 Full 3D mesh

Below is an extension of the relationship graphs Figure 3.5 between solar irradiation and wind speeds, and their resulting ΔT. The 3D mesh in Figure C.4 shows the combined relationship plots.

Figure C.4: 3D mesh showing the relationship between solar irradiation, wind speed and ΔT in one graph.

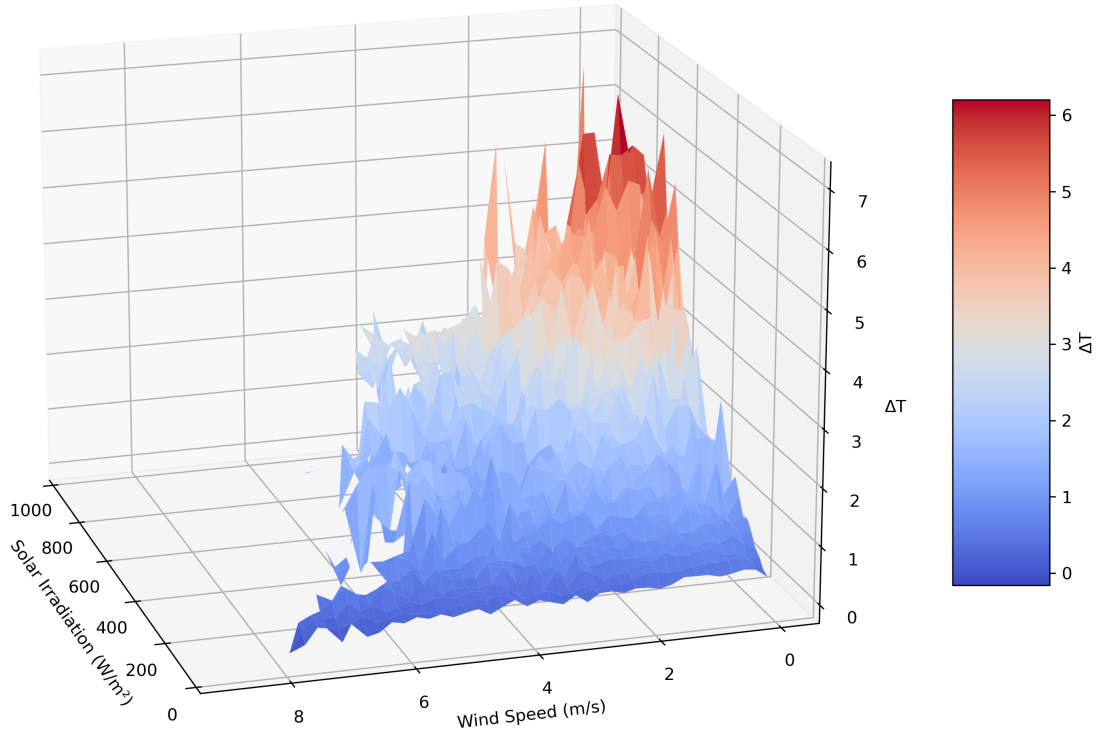

C.7 Spearman correlation analysis

A correlation analysis between the data sets has been attempted to understand better the relationship between temperature stratification and the environmental factors of wind speed and solar irradiation. Initially, it had been assumed that the general relation between the parameters is of a linear and monotonic nature, allowing the use of Spearman and Pearson correlations. Applying the correlation function for different brackets of the data, however, indicates a correlation way less than can be seen when manually evaluating that data.

Figure C.5: Spearman correlation between ΔT and solar irradiation (top) and wind speed (bottom) as brackets of the other.

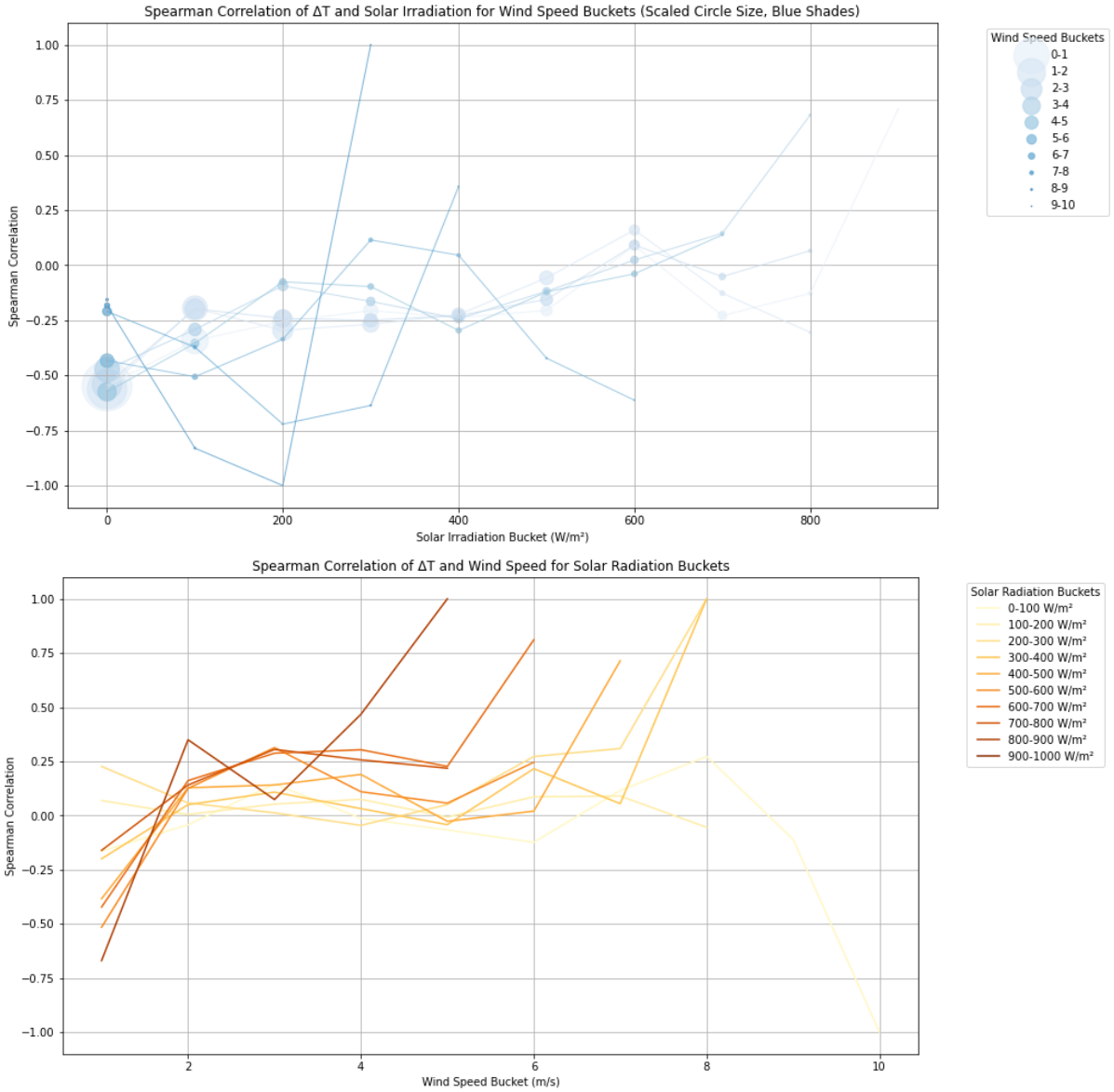

The plots in Figure C.5 show a negligible correlation, however. While the isolated ΔT and either parameter shows linear and largely monotonic relationships as shown in 3.5, the combination of all three parameters is neither linear nor monotonic anymore since increased solar irradiation and increased windspeeds have a reverse effect on the temperature stratification. The prediction model has since been made based on manual observations from the data. Solar irradiation is the main linear factor describing the relationship, with wind speed as a correction factor.

Appendix D

Appendix - BSim Model

D.1 Overview

Several models were created to see the impact of microclimate on buildings with different properties. In terms of size, three different models were made. One small office building which is 30m2 and has 4 occupants. A medium size office with 10 person and a large office of 160m2 with 20 occupants. Each of the models used the DRY 2010 and the DRY 2050 weather data file during the simulations to assess the impact of the microclimate on the energy consumption with the current weather conditions and provide a projection to the future. Once the baseline models were established and the validation process yielded a satisfactory result the impact of several temperature differences were analyzed. These temperature differences meant to mimic the microclimate where the ΔT was 0.5°C, 1°C, 1.5°C, 2°C, 2.5°C, 3°C and 3.5°C.

D.2 Model

The simulation software BSim includes a collection of advanced tools for simulating, among others, the thermal indoor climate, energy consumption, and daylight conditions [3]. To conclude a successful simulation, the following parameters had to be provided to BSim: Thermal properties, such as the heat transfer coefficients and insulation values. Environmental conditions, which in the case of this project, come in the form of the DRY2010 and DRY2050 weather files. Building geometry and orientation aimed to model different room sizes. Systems, such as heating or ventilation systems, are meant to maintain sufficient indoor environmental conditions, but also the internal loads, which are meant to represent the occupants, equipment, lighting, etc. Finally, the Occupancy patterns provide information about the usage of the occupied area.

However, to mimic the microclimate, a unique design had to be used during this project. Although the office sizes and the systems would vary between the three sizes, the main principle behind the layout of the models is the same. Each of the models consists of 4 rooms.

The Source room. This room aims to establish a certain temperature difference between the ambient air temperature and the internal air temperature within this room, thus mimicking the microclimate. Once the temperature difference is established, the air from this room is supplied directly to the occupied area (Target room) to see the effects of the temperature difference on the cooling coil´s energy consumption. To establish the desired temperature difference within the source room, a careful fine-tuning of the solar gains and the infiltration rate has to be found. The amount of solar gains entering this room can be adjusted by changing the size and the properties of the windows and skylights. All the windows and skylights have a Solar Transmittance value of 1, meaning that the entirety of solar radiation is allowed through them. The size of the source room is the equivalent size of the Occupied area. The following table aimed to summarize the magnitude of the infiltration rate and the window sizes for each of the three models to establish the desired temperature difference:

Table D.1: Summary of the changes made to establish the desired temperature difference in the Source room using the DRY2010 weather data file

ΔT	**Basic air change (/h), Small office**	**Window size, Small office (m2)**	**Basic air change (/h), Medium office**	**Window size, Medium office (m2)**	**Basic air change (/h), Large office**	**Window size, Large office (m2)**
0,5	250	4,2	250	8	200	16,6
1,0	80	4,2	85	8	80	16,6
1,5	40	4,2	40	8	35	16,6
2,0	15	4,2	20	8	15	16,6
2,5	5	4,2	8	8	7	16,6
3,0	1,5	4,2	3	8	2,5	16,6
3,5	0,1	4,2	0,1	8	0,5	16,6

Table D.2: Summary of the changes made to establish the desired temperature difference in the Source room using the DRY2050 weather data file

ΔT	**Basic air change (/h), Small office**	**Window size, Small office (m2)**	**Basic air change (/h), Medium office**	**Window size, Medium office (m2)**	**Basic air change (/h), Large office**	**Window size, Large office (m2)**
0,5	250	4,2	250	8	200	16,6
1,0	80	4,2	85	8	80	16,6
1,5	40	4,2	50	8	45	16,6
2,0	21	4,2	30	8	25	16,6
2,5	8	4,2	15	8	13	16,6
3,0	5	4,2	5	8	5	16,6
3,5	1,3	4,2	2	8	2	16,6

Not only does the model have a unique design, but the structural components of the source room itself are unique to counter the unwanted thermodynamic influence of certain layers. All the construction parts of the source room consist of three layers. A damp-proof membrane (Polyethylene) on the warm side of the wall to counter the effects of humidity. A 1cm thick concrete layer to serve as a placeholder for the window and the skylight. The reason behind a thin layer of concrete was due to mitigate the influence of the thermal mass of a concrete structure to the internal conditions. The final layer is 10cm thick mineral wool.

Table D.3: Material layers of the Source room

	Properties
Polyethylene	Damp-proof membrane
Concrete reinforced	Thickness 0,01m
Mineral wool 39	Thickness 0,1m

Thermal Buffer Zones. Two rooms are created between the Source room and the occupied area (Target room). These rooms serve as a buffer to counter any potential heat transfer between the Source room and the occupied area.

Target room. This part of the model was set up to re-create the occupied area, in case of this project three office spaces with different properties. The systems of this room contain Lighting, People load, venting, ventilation, and equipment loads. As described earlier, the ventilation system that supplies the air in this room uses the Source room as its air source. The construction elements of this room are using one of the most common constructions used in Denmark which also compiles with the current building regulations.

Table D.4: Material layers of the Target room

External wall	**Properties**
Concrete reinforced	Thickness 0,15m
Mineral wool 39	Thickness 0,125m
Brick external	Thickness 0,108m
U-value	0,27 W/m²K
Roof	
Concrete reinforced	Thickness 0,15m
Mineral wool 39	Thickness 0,35m
U-value	0,18 W/m²K
Floor	
Hardwood	Thickness 0,032m
Mineral wool 39	Thickness 0,2m
Concrete reinforced	Thickness 0,12m
U-value	0,17 W/m²K
Windows	
Solar Transmittance	0,56
Light Transmittance	0,74
U-value	1,3 W/m²K

Figure D.1: Small Office

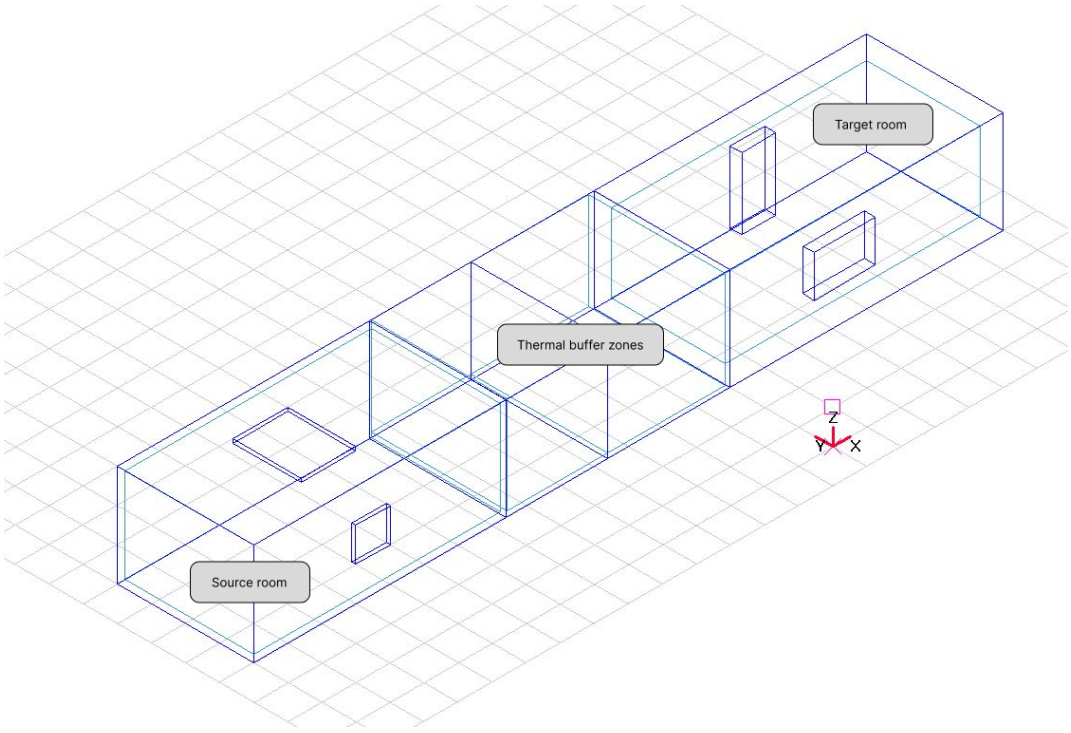

Figure D.2: Medium Office

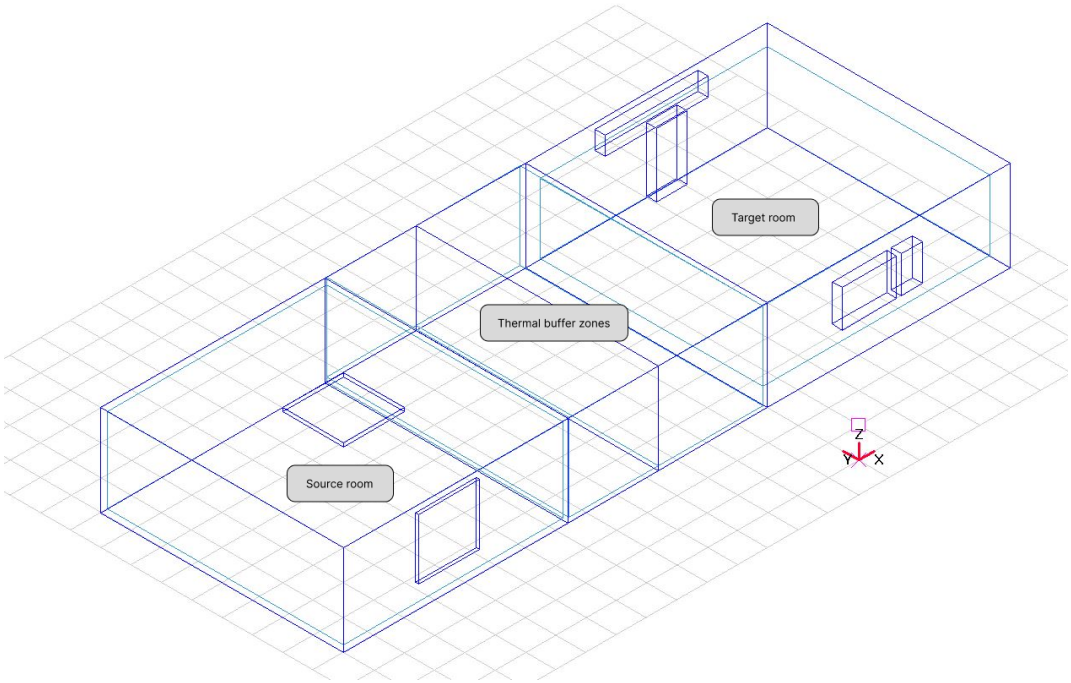

Figure D.3: Large Office

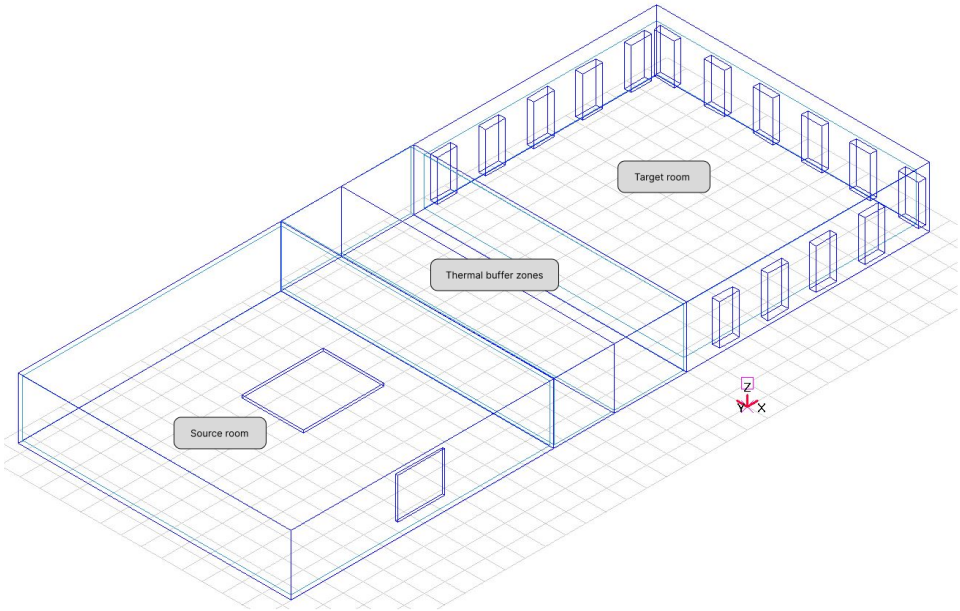

D.3 Systems

The three different offices are distinguishable from each other not only by their size but also by the internal loads and their systems. On the other hand, since the purpose of these simulations was to recreate the working environment within an office, the time span when the occupants are present is the same all over the three models. This schedule spans between 9:00 and 17:00 on weekdays all year long.
All the systems and internal loads used during the simulation can be found in the following table, separated to office sizes:

Table D.5: Systems of the Small Office

Lighting	**Properties**
Task Lightning	0,025 kW
General Lightning	0,25 kW
Gen. lightning Level	200 lux
Solar Limit	0,12 kW
Light control, factor	1
Light control, Lower Limit	0,1 kW
Light control, Temp. Max	26 °C
People load	
Number of People	4
Heat Generated	0,1 kW
Moisture Generated	0,06 kg/h
Dayprofile	100%9-12 100%14-17
Venting	
Basic AirChange	1 (/h)
TmpFactor	0,1 (/h/K)
TmpPower	0,5
WindFactor	0,1 (s/m/h)
Max AirChange	5 (/h)
VentingControl, Set Point	22,5 °C
Ventilation	
Input, Supply	0,07 m3/s
Input, Total Eff.	0,6
Input, Part to Air	0,6
Output, Return	0,07 m3/s
Output, Total Eff.	0,6
Output, Part to Air	0,6
Cooling Coil, Max Power	3 kW
Cooling Coil, Surf Temperature	16 °C
VAV Control, VAV max factor	1
VAV Control, Min Inlet Temp.	16 °C
VAV Control, Max Inlet Temp.	19 °C
VAV Control, Setp. Indoor Air	20 °C
VAV Control, Setp. Cooling	25 °C
VAV Control, Setp. CO2	1000 ppm
VAV Control, Air Humidity	0,07 kg/kg
Equipment	
Heat Load	0,5 kW
Part to air	0,5
Dayprofile	100%9-12 100%14-17

Table D.6: Systems of the Medium Office

Lighting	**Properties**
Task Lightning	0,054 kW
General Lightning	0,45 kW
Gen. lightning Level	200 lux
Solar Limit	0,12 kW
Light control, factor	1
Light control, Lower Limit	0,1 kW
Light control, Temp. Max	26 °C
People load	
Number of People	10
Heat Generated	0,1 kW
Moisture Generated	0,06 kg/h
Dayprofile	100%9-12 100%14-17
Venting	
Basic AirChange	3 (/h)
TmpFactor	0,1 (/h/K)
TmpPower	0,5
WindFactor	0,1 (s/m/h)
Max AirChange	5 (/h)
VentingControl, Set Point	22,5 °C
Ventilation	
Input, Supply	0,15 m3/s
Input, Total Eff.	0,6
Input, Part to Air	0,6
Output, Return	0,15 m3/s
Output, Total Eff.	0,6
Output, Part to Air	0,6
Cooling Coil, Max Power	3 kW
Cooling Coil, Surf Temperature	16 °C
VAV Control, VAV max factor	1
VAV Control, Min Inlet Temp.	16 °C
VAV Control, Max Inlet Temp.	19 °C
VAV Control, Setp. Indoor Air	20 °C
VAV Control, Setp. Cooling	25 °C
VAV Control, Setp. CO2	1000 ppm
VAV Control, Air Humidity	0,07 kg/kg
Equipment	
Heat Load	1 kW
Part to air	0,5
Dayprofile	100%9-12 100%14-17

Table D.7: Systems of the Large Office

Lighting	**Properties**
Task Lightning	0,1 kW
General Lightning	0,1 kW
Gen. lightning Level	200 lux
Solar Limit	0,12 kW
Light control, factor	1
Light control, Lower Limit	0,1 kW
Light control, Temp. Max	26 °C
People load	
Number of People	20
Heat Generated	0,1 kW
Moisture Generated	0,06 kg/h
Dayprofile	100%9-12 100%14-17
Venting	
Basic AirChange	3 (/h)
TmpFactor	0,1 (/h/K)
TmpPower	0,5
WindFactor	0,1 (s/m/h)
Max AirChange	5 (/h)
VentingControl, Set Point	22,5 °C
Ventilation	
Input, Supply	0,6 m3/s
Input, Total Eff.	0,6
Input, Part to Air	0,6
Output, Return	0,6 m3/s
Output, Total Eff.	0,6
Output, Part to Air	0,6
Cooling Coil, Max Power	3 kW
Cooling Coil, Surf Temperature	16 °C
VAV Control, VAV max factor	1
VAV Control, Min Inlet Temp.	16 °C
VAV Control, Max Inlet Temp.	19 °C
VAV Control, Setp. Indoor Air	20 °C
VAV Control, Setp. Cooling	25 °C
VAV Control, Setp. CO2	1000 ppm
VAV Control, Air Humidity	0,07 kg/kg
Equipment	
Heat Load	2 kW
Part to air	0,5
Dayprofile	100%9-12 100%14-17

D.4 Results

To assess the annual energy consumption of the cooling coil at a specific temperature difference, the results from the Heat Balance tab have to be exported. The parameter that provides information regarding the energy consumption of the cooling coil is the "ClCoil" row. This value provides the annual cooling coil energy consumption and breaks it down for each month. From BSim, these values are showcased in kWh. To properly compare the energy consumption of cooling coils of the three different offices, this value had to be divided by the size of the target rooms, thus converting the values in the unit of kWh/m2. This data was exported and summarized in an Excel table for each model at a specific temperature difference.

Table D.8: Annual energy consumption of the Small office, using the DRY2010 weather file

ΔT	**Annual energy consumption in kWh**	**Room size in m2**	**Annual energy consumption in kWh/m2**
0,0	136	30	4,5
0,5	152	30	5,1
1,0	178	30	6,0
1,5	201	30	6,7
2,0	225	30	7,5
2,5	254	30	8,5
3,0	281	30	9,4
3,5	301	30	10

Table D.9: Annual energy consumption of the Small office, using the DRY2050 weather file

ΔT	**Annual energy consumption in kWh**	**Room size in m2**	**Annual energy consumption in kWh/m2**
0,0	201	30	6,7
0,5	226	30	7,6
1,0	263	30	8,8
1,5	294	30	9,8
2,0	322	30	10,8
2,5	360	30	12,0
3,0	378	30	12,6
3,5	415	30	13,8

Table D.10: Annual energy consumption of the Medium office, using the DRY2010 weather file

ΔT	**Annual energy consumption in kWh**	**Room size in m2**	**Annual energy consumption in kWh/m2**
0,0	282	60	4,7
0,5	320	60	5,3
1,0	380	60	6,3
1,5	435	60	7,3
2,0	485	60	8,1
2,5	542	60	9,0
3,0	595	60	9,9
3,5	667	60	11,1

Table D.11: Annual energy consumption of the Medium office, using the DRY2050 weather file

ΔT	**Annual energy consumption in kWh**	**Room size in m2**	**Annual energy consumption in kWh/m2**
0,0	412	60	6,7
0,5	456	60	7,6
1,0	530	60	8,8
1,5	582	60	9,7
2,0	635	60	10,6
2,5	701	60	11,7
3,0	784	60	13,1
3,5	833	60	13,9

Table D.12: Annual energy consumption of the Large office, using the DRY2010 weather file

ΔT	**Annual energy consumption in kWh**	**Room size in m2**	**Annual energy consumption in kWh/m2**
0,0	3002	160	18,8
0,5	3410	160	21,3
1,0	3892	160	24,3
1,5	4459	160	27,9
2,0	5023	160	31,4
2,5	5462	160	34,1
3,0	5973	160	37,3
3,5	6446	160	40,3

Table D.13: Annual energy consumption of the Large office, using the DRY2010 weather file

ΔT	**Annual energy consumption in kWh**	**Room size in m2**	**Annual energy consumption in kWh/m2**
0,0	4437	160	27,7
0,5	4980	160	31,1
1,0	5648	160	35,3
1,5	6218	160	38,9
2,0	6835	160	42,7
2,5	7470	160	46,7
3,0	8242	160	51,5
3,5	8807	160	55,0

Afterwards, when the energy consumption of the cooling coil is converted to kWh/m2 the increase in energy consumption between a certain temperature differences can be calculated in a percent value. This value represent the difference between the baseline model using the DRY2010 weather file, when the temperature difference is 0 °C and all other scenarios when the temperature difference increases. This percentage value is used in the conversion table, serving as a database for the prediction tool which can render a % value showcasing the increase in energy consumption at a certain temperature difference.

Table D.14: Annual energy consumption of the Small office converted into % value to be used in the database. Using the DRY2010 weather file

ΔT	**Annual energy consumption in kWh/m2**	**Energy consumption increase compared to the baseline in %**
Baseline 0,0	4,5	-
0,5	5,1	12
1,0	6,0	31
1,5	6,7	48
2,0	7,5	67
2,5	8,5	87
3,0	9,4	107
3,5	10	122

Table D.15: Annual energy consumption of the Small office converted into % value to be used in the database. Using the DRY2050 weather file

ΔT	**Annual energy consumption in kWh/m2**	**Energy consumption increase compared to the baseline in %**
Baseline 0,0	4,5	-
0,5	7,6	68
1,0	8,8	95
1,5	9,8	118
2,0	10,8	139
2,5	12,0	167
3,0	12,6	179
3,5	13,8	208

Table D.16: Annual energy consumption of the Medium office converted into % value to be used in the database. Using the DRY2010 weather file

ΔT	**Annual energy consumption in kWh/m2**	**Energy consumption increase compared to the baseline in %**
Baseline 0,0	4,7	-
0,5	5,3	13
1,0	6,3	35
1,5	7,3	54
2,0	8,1	71
2,5	9,0	111
3,0	9,9	136
3,5	11,1	163

Table D.17: Annual energy consumption of the Medium office converted into % value to be used in the database. Using the DRY2050 weather file

ΔT	**Annual energy consumption in kWh/m2**	**Energy consumption increase compared to the baseline in %**
Baseline 0,0	4,7	-
0,5	7,6	62
1,0	8,8	88
1,5	9,7	107
2,0	10,6	125
2,5	11,7	148
3,0	13,1	178
3,5	13,9	196

Table D.18: Annual energy consumption of the Large office converted into % value to be used in the database. Using the DRY2010 weather file

ΔT	**Annual energy consumption in kWh/m2**	**Energy consumption increase compared to the baseline in %**
Baseline 0,0	18,8	-
0,5	21,3	14
1,0	24,3	29
1,5	27,9	49
2,0	31,4	67
2,5	34,1	82
3,0	37,3	99
3,5	40,3	115

Table D.19: Annual energy consumption of the Large office converted into % value to be used in the database. Using the DRY2050 weather file

ΔT	**Annual energy consumption in kWh/m2**	**Energy consumption increase compared to the baseline in %**
Baseline 0,0	18,8	-
0,5	31,1	66
1,0	35,3	88
1,5	38,9	107
2,0	42,7	127
2,5	46,7	148
3,0	51,5	174
3,5	55,0	192

To assess the Cooling coil's peak load under the parameters tab, the ClCoil Ventilation Component is exported. This provides the hourly average value of the cooling coil in kW for the entire year. A code in Python was used to assess this large quantity of data. The code assessing the data for the entire year, filtering out the days where the energy consumption of the cooling coil is 0 kW and only considering the time when the coil is in usage. These days are than sorted in a descending order from the specific hour of the year when the cooling coil uses the largest amount of energy to the hour when it is the lowest. Since the Building Regulation only only allows the maximum of 25 hours above 27 °C, the 25th hour when the cooling coil energy consumption is the highest is considered to be the peak. Once this value is found, the peak energy consumption of the cooling coil is also included in the conversion table in a % value showcasing the increase in energy consumption between the baseline model, when the temperature difference is 0 °C, using the DRY2010 weather file and all other scenarios when the temperature difference increases. Thus providing a combined database for the prediction tool where both the annual energy consumption and the peak energy consumption showcasing the increase in energy consumption at a certain temperature difference in a % value.

Table D.20: Peak energy usage of the Small office converted into % value to be used in the database. Using the DRY2010 weather file

ΔT	**Peak energy consumption in kW**	**Peak Energy consumption increase compared to the baseline in %**
Baseline 0,0	0,79	-
0,5	0,85	8
1,0	0,91	15
1,5	0,97	23
2,0	1,05	33
2,5	1,12	42
3,0	1,18	49
3,5	1,22	54

Table D.21: Peak energy usage of the Small office converted into % value to be used in the database. Using the DRY2050 weather file

ΔT	**Peak energy consumption in kW**	**Peak Energy consumption increase compared to the baseline in %**
Baseline 0,0	0,79	-
0,5	1,34	70
1,0	1,44	82
1,5	1,5	90
2,0	1,56	98
2,5	1,65	109
3,0	1,7	115
3,5	1,75	122

Table D.22: Peak energy usage of the Medium office converted into % value to be used in the database. Using the DRY2010 weather file

ΔT	**Peak energy consumption in kW**	**Peak Energy consumption increase compared to the baseline in %**
Baseline 0,0	1,72	-
0,5	1,82	6
1,0	2,00	16
1,5	2,13	24
2,0	2,27	32
2,5	2,41	40
3,0	2,54	48
3,5	2,68	56

Table D.23: Peak energy usage of the Medium office converted into % value to be used in the database. Using the DRY2050 weather file

ΔT	**Peak energy consumption in kW**	**Peak Energy consumption increase compared to the baseline in %**
Baseline 0,0	1,72	-
0,5	2,81	63
1,0	3,04	76,7
1,5	3,20	86
2,0	3,25	89
2,5	3,47	102
3,0	3,66	113
3,5	3,67	114

Table D.24: Peak energy usage of the Large office converted into % value to be used in the database. Using the DRY2010 weather file

ΔT	**Peak energy consumption in kW**	**Peak Energy consumption increase compared to the baseline in %**
Baseline 0,0	18,14	-
0,5	19,88	10
1,0	21,77	20
1,5	24,95	38
2,0	26,08	44
2,5	27,26	50
3,0	29,30	62
3,5	30,46	67,9

Table D.25: Peak energy usage of the Large office converted into % value to be used in the database. Using the DRY2050 weather file

ΔT	**Peak energy consumption in kW**	**Peak Energy consumption increase compared to the baseline in %**
Baseline 0,0	18,14	-
0,5	30,31	67
1,0	32,48	79
1,5	34,87	92
2,0	36,94	104
2,5	38,97	115
3,0	41,44	128
3,5	42,87	136

After assessing the peak energy consumption of the cooling coil, not only the energy consumption increases in relation with the temperature difference but the operational period when the coil is in usage also extends. The summary of this can be observed in the tables below:

Table D.26: Peak energy usage of the Small office and the operation period of the cooling coil. Using the DRY2010 weather file

ΔT	**Peak enegy consumption in kW**	**Cooling coil operational period**
0,0	0,79	2010-4-29 14h - 2010-9-22 16h
0,5	0,85	2010-4-29 14h - 2010-9-22 17h
1,0	0,91	2010-4-29 13h - 2010-9-22 17h
1,5	0,97	2010-4-29 13h - 2010-9-22 17h
2,0	1,05	2010-4-29 14h - 2010-9-22 17h
2,5	1,12	2010-4-28 14h - 2010-9-23 16h
3,0	1,18	2010-4-14 16h - 2010-10-12 16h
3,5	1,22	2010-4-14 16h - 2010-10-12 16h

Table D.27: Peak energy usage of the Small office and the operation period of the cooling coil. Using the DRY2050 weather file

ΔT	**Peak enegy consumption in kW**	**Cooling coil operational period**
0,0	1,28	2050-4-28 14h - 2050-9-29 15h
0,5	1,34	2050-4-22 15h - 2050-9-29 17h
1,0	1,44	2050-4-22 14h - 2050-10-17 16h
1,5	1,50	2050-4-22 13h - 2050-10-19 15h
2,0	1,56	2050-4-22 13h - 2050-10-19 17h
2,5	1,65	2050-4-22 13h - 2050-10-20 17h
3,0	1,70	2050-4-19 16h - 2050-10-20 17h
3,5	1,75	2050-4-18 16h - 2050-10-20 17h

Table D.28: Peak energy usage of the Medium office and the operation period of the cooling coil. Using the DRY2010 weather file

ΔT	**Peak enegy consumption in kW**	**Cooling coil operational period**
0,0	1,72	2010-4-29 14h - 2010-9-22 16h
0,5	1,82	2010-4-29 13h - 2010-9-22 17h
1,0	2,00	2010-4-29 13h - 2010-9-22 17h
1,5	2,13	2010-4-29 13h - 2010-9-22 17h
2,0	2,27	2010-4-29 13h - 2010-10-8 15h
2,5	2,41	2010-4-15 16h - 2010-10-14 15h
3,0	2,54	2010-4-14 15h - 2010-10-14 17h
3,5	2,68	2010-4-7 16h - 2010-10-14 17h

Table D.29: Peak energy usage of the Medium office and the operation period of the cooling coil. Using the DRY2050 weather file

ΔT	**Peak enegy consumption in kW**	**Cooling coil operational period**
0,0	2,67	2050-4-28 14h - 2050-9-29 15h
0,5	2,81	2050-4-22 15h - 2050-9-29 17h
1,0	3,04	2050-4-22 13h - 2050-10-17 16h
1,5	3,20	2050-4-22 13h - 2050-10-19 16h
2,0	3,25	2050-4-22 13h - 2050-10-19 17h
2,5	3,47	2050-4-22 13h - 2050-10-20 17h
3,0	3,66	2050-4-18 16h - 2050-10-21 16h
3,5	3,67	2050-4-18 15h - 2050-10-21 17h

Table D.30: Peak energy usage of the Large office and the operation period of the cooling coil. Using the DRY2010 weather file

ΔT	**Peak enegy consumption in kW**	**Cooling coil operational period**
0,0	18,14	2010-4-29 14h - 2010-9-22 16h
0,5	19,88	2010-4-29 13h - 2010-9-22 17h
1,0	21,77	2010-4-29 13h - 2010-9-22 17h
1,5	24,95	2010-4-29 13h - 2010-9-22 17h
2,0	26,08	2010-4-29 13h - 2010-9-22 17h
2,5	27,26	2010-4-28 14h - 2010-9-23 16h
3,0	29,30	2010-4-14 16h - 2010-10-8 17h
3,5	30,46	2010-4-14 15h - 2010-10-14 16h

Table D.31: Peak energy usage of the Large office and the operation period of the cooling coil. Using the DRY2050 weather file

ΔT	**Peak enegy consumption in kW**	**Cooling coil operational period**
0,0	29,38	2050-4-28 14h - 2050-9-29 15h
0,5	30,31	2050-4-22 15h - 2050-9-29 17h
1,0	32,48	2050-4-22 14h - 2050-9-29 17h
1,5	34,87	2050-4-22 13h - 2050-10-17 17h
2,0	36,94	2050-4-22 13h - 2050-10-19 16h
2,5	38,97	2050-4-22 13h - 2050-10-19 17h
3,0	41,44	2050-4-18 16h - 2050-10-20 17h
3,5	42,81	2050-4-18 16h - 2050-10-20 17h

Appendix E

Appendix - Prediction tool

In this appendix, the functions and setup of the prediction tool will be described in detail, pointing out all functions used, all filters applied to the measurement data and weather data for the application within the tool, and all assumptions that need to be met. Finally, the list of regression models per channel will be shown, as well as the Python code of the tool as a whole.

E.1 Data filters

The data used for training purposes for the model has been filtered to allow precise predictions without outliers distorting the result. From the raw data (measurements), firstly, all data has been turned into minute averages to account for the different time constants of the sensors (all are below one minute). Temperature filters have been applied for the range of 5°C - 33°C to remove any potentially faulty measurements.

E.1.1 Wind profile adjustment

For both locations of PON and TMV, only rows with complete data, meaning a valid wind speed, a valid solar irradiation and valid temperature data for all 8 channels has been considered. Next, the wind speed for both locations has been adjusted based on their roughness length and building height with the following parameters:

- $z_{0_{\mathrm{PON}}} = 1$
- $z_{1_{\mathrm{PON}}} = 4.5$
- $z_{0_{\mathrm{TMV}}} = 0.3$
- $z_{1_{\mathrm{TMV}}} = 15$

Where z0 is the roughness length, and z1 is the building height. The roughness length at pon has been chosen as 1 meter since it is surrounded by 1-2 story buildings, resembling a suburban area. Conversely, TMV is the largest building in its direct vicinity, with fields and shallow hills surrounding it, making it a lot more wind-exposed. For the building heights, the height from the surrounding ground level to the roof surface has been chosen. No further adjustment based on the height of each channel has been made in the code since wind speed has been measured at one height anyway.

E.2 Files used for tool

The following files are used within the prediction tool:

Table E.1: Data files used in prediction tool

File Name	Used for	Filters
Training_data.csv	Base training data consisting of combined and filtered temperature, solar irradiation, and wind speed data from TMV and PON	Filters described above
Dry2010clean.csv	Standardized Danish weather data file applicable to the whole of Denmark. Used for predictions after training is complete	N/A
conversionTable.csv	Summarizes results of building energy analysis. Used for conversion from predicted ΔT to annual and peak energy demand impact	N/A

When running the code on a local environment, the file paths need to be adjusted to wherever these files have been saved.

E.3 Selection of Model

During the development phase of the prediction tool, various models have been considered to predict the temperatures in the microclimate. Firstly, a machine learning-based algorithm called XGBoost was attempted. After fitting all model hyperparameters to reduce the error, the model has been trained on the measurement data—however, too high MAEs when switching from one site's data to another stopped development. Next, a multivariable polynomial regression model has been tried out since a mix of linear and quadratic relations between the three primary parameters of the model were observed. After training and testing this model, too strong overfitting has been identified when applying the model to the external weather data set for predictions. Lastly, a simple linear regression has been tried despite the slight exponential relations found in the data. This model is primarily based on the connection between temperature stratification and solar irradiation, with a wind speed and a unitless linear correction factor adjusting the model. This model is convinced with its low mean error, and across the 3 models created, it also shows the lowest MAE. A total of 7 equations have been fitted to the raw data shown below.

E.3.1 Equations used in regression

The following equations are used per channel to predict the temperatures in the microclimate:

$$\Delta T_{Ch.1} = 0.00392 \cdot \text{Solar} - 0.03 \cdot \text{Wind} + 0.42358 \tag{E.1}$$

$$\Delta T_{Ch.2} = 0.00584 \cdot \text{Solar} - 0.10 \cdot \text{Wind} + 0.08403 \tag{E.2}$$

$$\Delta T_{Ch.3} = 0.00419 \cdot \text{Solar} - 0.04 \cdot \text{Wind} + 0.00279 \tag{E.3}$$

$$\Delta T_{Ch.4} = 0.00277 \cdot \text{Solar} - 0.07 \cdot \text{Wind} + 0.15242 \tag{E.4}$$

$$\Delta T_{Ch.5} = 0.00214 \cdot \text{Solar} - 0.04 \cdot \text{Wind} + 0.01287 \tag{E.5}$$

$$\Delta T_{Ch.6} = 0.00194 \cdot \text{Solar} - 0.07 \cdot \text{Wind} - 0.00990 \tag{E.6}$$

$$\Delta T_{Ch.7} = 0.00042 \cdot \text{Solar} - 0.02 \cdot \text{Wind} + 0.07526 \tag{E.7}$$

E.4 Prediction tool python code

```
import pandas as pd
from sklearn.model_selection import train_test_split
from sklearn.linear_model import LinearRegression
from sklearn.metrics import mean_absolute_error
import numpy as np
import warnings

inlet_height = 150 # Mean level of inlet height above roof.

# User-specified wind profile parameters
Roughness_Length_User = 1   # Specify Roughness length of your buildings surroundings.
Building_Height_User = 5   # Enter the height of your building in Meter. Distance from groundlevel till roof plain where AHU is positioned.

# Table with different roughness lengths from "Updating the Davenport roughness classification" by Jon Wieringa
# Sea, loose sand and snow = 0,0002
# Concrete, flat desert, tidal flat = 0.0002-0.0005
# Flat snow field = 0.0001-0.0007
# Rough Ice field = 0.001-0.012
# Fallow ground = 0.001-0.004
# Short grass and moss = 0.008-0.03
# Long grass and heather = 0.02-0.06
# Low mature agricultural crops = 0.04-0.09
# High mature crops ("grain") = 0.12-0.18
# Continuous bushland = 0.35-0.45
# Mature pine forest = 0.8-1.6
# Dense low buildings ("suburb") = 0.4-0.7
# Regularly-built large town = 0.7-1.5
# Tropical forest = 1.7-2.3

#Determine Time range for predictions. Choose start and end month, as well as start and end time.
Start_Month = 6
End_Month = 9
Start_Time = 8
End_Time = 18
Training_data_size = 1 # 1 = 100% of data is used for training & 0 = 0% is used.

# Define the channel heights mapping
channel_heights = {
    1: 5,   # Ch. 1 = 5 cm
    2: 10,  # Ch. 2 = 10 cm
    3: 20,  # Ch. 3 = 20 cm
    4: 30,  # Ch. 4 = 30 cm
    5: 40,  # Ch. 5 = 40 cm
    6: 50,  # Ch. 6 = 50 cm
    7: 100, # Ch. 7 = 100 cm
    8: 200  # Ch. 8 = 200 cm, ambient temperature
}

# Path to training data. Replace with location where "Training_data.csv" is stored.
data = pd.read_csv('your_path/Training_data.csv')

# Path to weather data. Replace with location where "Dry2010clean.csv" is stored.
# If other weather data is to be used, ensure the column headers per parameter are identical to the column headers in "Dry2010clean.csv".
dry_data = pd.read_csv('your_path/Dry2010clean.csv')

# Load the conversion table
conversion_table = pd.read_csv('your_path/conversionTable.csv')

# Preperation of trianing Data
# Calculate DeltaT for each channel
for i in range(1, 8):  # Channels 1 to 7
    delta_column_name = f'DeltaT_Ch{i}'
    data[delta_column_name] = data[f'Ch. {i}'] - data['Ch. 8']

# Prepare the features (Solar Irradiation and Wind Speed) and target (DeltaT for each channel)
```

```
features = ['Solar', 'Wind']
targets = [f'DeltaT_Ch{i}' for i in range(1, 8)]

# Splitting the data into train and test sets
train, test = train_test_split(data, test_size=1.001 - Training_data_size, random_state=1)

# Training a model for each channel and collecting mean errors
mean_errors_mae = {}
mean_errors_normal = {}
models = {}
for target in targets:
    # Prepare training data
    X_train = train[features]
    y_train = train[target]
    X_test = test[features]
    y_test = test[target]

    # Initialize and train the model
    model = LinearRegression()
    model.fit(X_train, y_train)
    models[target] = model  # Storing model for future predictions

    # Make predictions and evaluate the model
    predictions = model.predict(X_test)

    # Calculate both MAE and normal mean error
    mae = mean_absolute_error(y_test, predictions)
    mean_errors_mae[target] = round(mae, 2)  # MAE rounded to 2 decimal places

    error = np.mean(predictions - y_test)  # Calculate normal mean error
    mean_errors_normal[target] = round(error, 2)  # Normal mean error rounded to 2 decimal places

# Applying DateTime filters to Weather data file
dry_data = dry_data[(dry_data['Month'] >= Start_Month) & (dry_data['Month'] <= End_Month) & (
    dry_data['Hour'] >= Start_Time) & (dry_data['Hour'] <= End_Time)]

# Rename Weather Data column headers to match naming structure of training data
dry_data.rename(columns={'Solar Irradiation': 'Solar', 'Wind Speed': 'Wind', 'Ch. 8': 'Temperature
    '}, inplace=True)

# Account for inlet height in wind profile adjustment
h = Building_Height_User + inlet_height / 10

#Adjust wind speed for wind site specific wind profile
def adjust_wind_speed(Vref, h, Roughness_Length_User, href=10, rref=0.3):
    if h <= 0 or Roughness_Length_User <= 0 or href <= 0 or rref <= 0:
        raise ValueError("Heights and roughness length must be positive.")
    try:
        adjusted_speed = Vref * (np.log(h / Roughness_Length_User) / np.log(href / rref))
        return adjusted_speed
    except ZeroDivisionError:
        raise ValueError("Error in wind profile calculation - check input values.")

user_scenario_data = dry_data.copy()
user_adjusted_wind_speed = adjust_wind_speed(user_scenario_data['Wind'], Building_Height_User,
    Roughness_Length_User)
user_scenario_data['Wind'] = user_adjusted_wind_speed

# Predict DeltaT for each channel and calculate the channel temperatures
predicted_temps = pd.DataFrame()
for target in targets:
    # Predicting DeltaT using the model for each channel
    predicted_DeltaT = models[target].predict(dry_data[features])
    channel = target.split('_')[-1]  # e.g., 'Ch1'
    # Calculate predicted channel temperature and store it
    predicted_temps[channel] = dry_data['Temperature'] + predicted_DeltaT  # No 'Predicted_'
    prefix

# Calculate mean predicted temperature for each channel including the ambient temperature
mean_predicted_temps = predicted_temps.mean(axis=0)

```

```
# Recalculate predicted temperatures using adjusted wind speeds
user_predicted_temps = pd.DataFrame()
for target in targets:
    predicted_DeltaT = models[target].predict(user_scenario_data[features])
    channel = target.split('_')[-1]
    user_predicted_temps[channel] = predicted_DeltaT

# Setting Ch. 8 temperature to 0 since it represent the ambient temperature
user_predicted_temps['Ch8'] = 0

# Calculate mean predicted temperature for each channel
mean_user_predicted_temps = user_predicted_temps.mean(axis=0)

# Interpolate predicted temperatures between channels
def interpolate_temperature(inlet_height, channel_heights, mean_user_predicted_temps):
    heights = np.array(list(channel_heights.values()))
    temps = np.array([mean_user_predicted_temps[f'Ch{i}'] for i in channel_heights.keys()])

    # Select indices for interpolation
    indices = np.argsort(np.abs(heights - inlet_height))[:3]  # Initial selection of three closest heights

    # Ensure inclusion of 200 cm for heights significantly close to it
    if inlet_height > 100:
        indices = np.argsort(np.abs(heights - inlet_height))[:2]
        indices = np.append(indices, 7)  # Append index of 200 cm (ambient temperature)

    closest_heights = heights[indices]
    closest_temps = temps[indices]

    # Perform 2nd degree polynomial interpolation, handle RankWarning
    try:
        with warnings.catch_warnings():
            warnings.simplefilter("ignore", np.RankWarning)  # Suppress RankWarning
            # Fit a 2nd-degree polynomial to the points
            interpolation_function = np.poly1d(np.polyfit(closest_heights, closest_temps, 2))
        # Use the interpolation function to find the interpolated temperature
        interpolated_temp = interpolation_function(inlet_height)
    except Exception as e:
        print("An error occurred during interpolation:", e)
        interpolated_temp = np.nan

    return interpolated_temp

# Function to interpolate MAE or Mean Error based on the inlet height using linear interpolation
def interpolate_error(inlet_height, channel_heights, error_values):
    heights = np.array(list(channel_heights.values()))  # Use all channel heights
    errors = np.array([error_values.get(f'DeltaT_Ch{i}', 0) for i in range(1, len(channel_heights) + 1)])  # Use 0 for Ch. 8

    # Select indices for interpolation
    indices = np.argsort(np.abs(heights - inlet_height))[:3]  # Initial selection of three closest heights

    # Ensure inclusion of 200 cm for heights significantly close to it
    if inlet_height > 100:
        indices = np.argsort(np.abs(heights - inlet_height))[:2]
        indices = np.append(indices, 7)  # Append index of 200 cm (ambient temperature)

    closest_heights = heights[indices]
    closest_errors = errors[indices]

    # Sort by heights for linear interpolation
    sort_indices = np.argsort(closest_heights)
    closest_heights = closest_heights[sort_indices]
    closest_errors = closest_errors[sort_indices]

    # Linear interpolation
    interpolated_error = np.interp(inlet_height, closest_heights, closest_errors)

    return interpolated_error
```

```
201
202 # Now, you can use this function to calculate the interpolated MAE and Mean Error
203 interpolated_mae = interpolate_error(inlet_height, channel_heights, mean_errors_mae)
204 interpolated_mean_error = interpolate_error(inlet_height, channel_heights, mean_errors_normal)
205
206 # Find the corresponding channel for the inlet height
207 channel_number = None
208 for ch, height in channel_heights.items():
209     if height == inlet_height:
210         channel_number = ch
211         break
212
213 # Calculate interpolated temperature or use the channel temperature
214 if channel_number is None:
215     interpolated_temp = interpolate_temperature(inlet_height, channel_heights,
    mean_user_predicted_temps)
216 else:
217     # Use the channel number to fetch the predicted mean temperature
218     inlet_channel = f'Ch{channel_number}'
219     interpolated_temp = mean_user_predicted_temps[inlet_channel]
220
221 # Now you can print the predicted temperature, MAE, and Mean Error
222 print(f"Predicted mean temperature at {inlet_height} cm is: {interpolated_temp:.2f} C ")
223 print(f"MAE: {interpolated_mae:.2f} C ")
224 print(f"Mean Error: {interpolated_mean_error:.2f} C ")
225
226 # Building sizes to loop through
227 sizes = ['s', 'm', 'l']
228
229 # Function to interpolate percentages based on DeltaT
230 def interpolate_conversion(delta_t, section):
231     delta_t = float(delta_t)  # Ensure delta_t is a float
232     delta_ts = section['Delta T'].values
233     annual_savings = section['2010 Annual'].values
234     peak_savings = section['2010 Peak'].values
235
236     annual_percentage = np.interp(delta_t, delta_ts, annual_savings)
237     peak_percentage = np.interp(delta_t, delta_ts, peak_savings)
238
239     return annual_percentage, peak_percentage
240
241 # Initialize a dictionary to hold the results
242 results = {size: {} for size in sizes}
243
244 # Calculate and store interpolated percentages for all building sizes
245 for size in sizes:
246     # Filter the data for the current size
247     section = conversion_table[conversion_table['Size'] == size]
248     annual_percentage, peak_percentage = interpolate_conversion(interpolated_temp, section)
249     results[size] = {
250         'Annual': annual_percentage,
251         'Peak': peak_percentage
252     }
253
254 # Printing the results in a table format
255 print()
256 print("Impact on energy demand of buildings with different sizes. For details on building
    properties, see Appendix D")
257 print(f"{'Building Size':<15}{'Annual (%)':<15}{'Peak (%)':<15}")
258 for size, res in results.items():
259     print(f"{size.upper():<15}{res['Annual']:.2f}{'%':<13}{res['Peak']:.2f}%")
```

E.5 Assumptions to use the prediction tool

Since the prediction tool is based on a black box model, the characteristics of the target roof need to closely resemble the characteristics of the roofs used for training data. This means that it needs to be positioned in roughly the same climatic conditions, the roof needs to be covered with a material of the same albedo as the training roof and there must be no shade on the analyzed section of the roof. Failure to meet these assumptions may result in the

predictions made by the tool being unreliable since most of these variables have not been trained for.

Appendix F

Appendix - Prediction Tool user guide

The prediction tool is intended to be used by other engineers for their design evaluations to be aware of the energy demand implications of HVAC unit positioning if they are placed on top of the building roof. This appendix describes how the tool needs to be set up to function in a local environment and which customization options are available to the user.

The attached Python file "Prediction Tool.py" needs to be run in a suitable environment like "Spyder". Once opened, the connections to the data files need to be established by entering the file path of where they have been placed. To receive the file path, select the file in the file explorer, press "Ctrl + Shift + C" (for Windows), and past the paths into the following lines in the code:

```
data = pd.read_csv('Path to training data')
dry_data = pd.read_csv('Path to DRY2010 weather data')
conversion_table = pd.read_csv('Path to conversion table')
```

Ensure that all "\" are replaced with "/" for python to be able to understand the file path.

If a different weather data file as a basis for predictions is used than the DRY 2010 weather data file, ensure that the column headers are matching the original file:

Year	Month	Day	Hour	Solar Irradiation	Wind Speed	Ch. 8

Table F.1: Column headers used for weather data file

Install all needed packages for your environment:

- pandas: For data manipulation and analysis.
- scikit-learn: For machine learning algorithms and model evaluation metrics.
- numpy: For numerical computing.

Next, the the building and prediction parameters can be adjusted to receive a customized prediction. The parameters include the following:

Parameter	Function	Note
inlet_height	Defines the inlet height for which the prediction is made. Choose the average level of your inlet duct from the roof-mounted HVAC unit.	Must be between 5 and 200 cm as this is the range for which training data is available. Results for inlet heights between measured channel heights are polynomially interpolated based on the surrounding channels.
Roughness_Length_User	Defines the roughness length of the case building's surroundings. Used for wind profile correction.	Choose a suitable scenario from the provided table in the code. Higher roughness lengths mean lower wind speeds and vice versa.
Building_Height_User	Defines the case building height in meters. The height difference from the surrounding ground level to the roof level on which the HVAC unit is positioned.	Higher building heights result in higher wind speeds according to the logarithmic wind profile law.
Start_Month	Defines the start month of the prediction period. The selected month is included.	Allows predictions for specific months or seasons only.
End_Month	Defines the end month of the prediction period. The selected month is included.	Allows predictions for specific months or seasons only.
Start_Time	Defines the start time of the prediction period. Given in hours, based on a 24-hour clock.	Allows predictions for specific times of the day. Ideally, choose operation hours of the cooling coil.
End_Time	Defines the end time of the prediction period. Given in hours, based on a 24-hour clock.	Allows predictions for specific times of the day. Ideally, choose operation hours of the cooling coil.
Training_data_size	Percentage of data used for training. Range between 0-1.	A higher number results in higher prediction accuracy.

Table F.2: Description of Input Parameters for the Prediction Model

After running the tool, the output looks as follows:

Predicted mean temperature at "inlet_height" cm is: x.xx°C
MAE: x.xx°C
Mean Error: x.xx°C
Impact on energy demand of buildings with different sizes. For details on building properties, see Appendix D

Building Size	Annual (%)	Peak (%)
S	x.xx%	x.xx%
M	x.xx%	x.xx%
L	x.xx%	x.xx%

The annual and peak energy demand changes are attempts at predicting the potential influence of the microclimate temperature stratification on a cooling coil inside an HVAC unit and are only an estimation. Precise modeling of the actual case building is needed to receive case-specific energy demand impact values.

Appendix G

Appendix - Arduino Code

This code was developed and used for data logging so all the necessarily temperature data and wind speed can be recorded. The Arduino code was written in the Arduino Integrated Development Environment (IDE). Through this program, the code was uploaded to the Arduino Mega Boards. This code is capable of measuring 11 temperature channels, and through the connection of an Anemometer, it logs the wind speed and wind direction every 4 seconds. As a disclaimer, although indicated but the current code is unable to be integrated and log solar radiation from a Pyranometer. Due to continuous setbacks during the development phase, the integration of this instrument was halted and later completely canceled. Instead an external setup was connected to a Pyranometer from which the data was extracted by using a USD data logger.

G.1 Libraries used

In order to successfully integrate and run this code, the following liberias have to be included:

Table G.1: Arduino libaries and its function

Libaries	Functions
SD.h	Used for reading from and writing to the SD card
Adafruit MAX31865.h	This library is designed for the Adafruit MAX31865 board, which is a thermocouple amplifier. The library simplifies the process of reading temperatures from these sensors.
Wire.h	This is a library for I2C communication, a common communication protocol.
RTClib.h	This library is used for interfacing with Real Time Clock (RTC) modules

G.2 Constants

The following constants and their functions are present in the code. SD CS (53), which defines the pin number for the SD card module. FILENAME ("arduino2.csv"), this is the specific file name to be created by the SD card for datalogging. RREF (430.0), is the resistance value used in calculations with the MAX31865 RTD-to-digital converter. RNOMINAL (100.0) represents the RTD sensor's nominal resistance, typically 100 ohms for the pt100 sensors. V REF (5.0) is the reference voltage for the Arduino board. ANEMOMETER WIND SPEED PIN (A0) and ANEMOMETER WIND DIRECTION PIN (A1), are the analog pins to which wind speed and wind direction sensors are connected.

G.3 Initialization and setup

The "void setup" initializes settings and configures the pins once the logging commences. For debugging and logging the 9600 bound rate was chosen. Some of its main operations include beginning the communication with the Real Time Clock (RTC) module, initializing each of the 11 thermocouple amplifiers, and signaling to the SD card reader, it commences the data file creation.

G.4 Main program logic and data logging

The ”void loop” function is responsible for the continuous running of the main logic of the program once the ”void setup” initializes the settings. As part of the void loop, the ”initSDCard()” function manages the creation, opening, and writing of the logged data on the SD card. The logged data includes the date-time, the temperature readings the wind speed, and wind directions. Furthermore within the void loop and the initSDCard() function, the error handling, such as re-initialization of the SD card or the printing of the error message on the serial monitor, takes place.

G.5 Arduino code

The full code of the Arduino setup used during the measurement campaign can be found below:

```
#include <SD.h>
#include <Adafruit_MAX31865.h>
#include <Wire.h>
#include "RTClib.h"

#constants and access pins
#define SD_CS 53
#define FILENAME "arduino2.csv"
#define RREF 430.0
#define RNOMINAL 100.0
#define AMP_OUTPUT_PIN A2
#define ADC_MAX 1023.0
#define V_REF 5.0
#define ANEMOMETER_WIND_SPEED_PIN A0
#define ANEMOMETER_WIND_DIRECTION_PIN A1

#pin layout
// Thermocouple Amplifiers
Adafruit_MAX31865 thermo[11] = {
  {46, 47, 48, 49},
  {45, 47, 48, 49},
  {44, 47, 48, 49},
  {43, 47, 48, 49},
  {42, 47, 48, 49},
  {41, 47, 48, 49},
  {40, 47, 48, 49},
  {39, 47, 48, 49},
  {38, 47, 48, 49},
  {37, 47, 48, 49},
  {36, 47, 48, 49},
};

#new file creation and clock
// Global variables for file and RTC
File myFile;
RTC_DS3231 rtc;

#start up the SD card and printing the headers if they are not already present
// Variables for the Pyranometer
const int numReadings = 5;
float readings[numReadings];
int readIndex = 0;
float total = 0;
float average = 0;

bool initSDCard() {
  if (!SD.begin(SD_CS)) {
    Serial.println(F("SD card failed, or not present"));
    return false;
  }
  Serial.println(F("SD card initialized."));
  if (!SD.exists(FILENAME)) {
    Serial.println(String(FILENAME) + " doesn't exist. Creating file...");
    myFile = SD.open(FILENAME, FILE_WRITE);
    if (myFile) {
```

```
      myFile.println("DateTime, Ch. 1, Ch. 2, Ch. 3, Ch. 4, Ch. 5, Ch. 6, Ch. 7, Ch. 8, Ch. 9, Ch. 10, Ch. 11, Voltage, Irradiance, Wind Speed, Wind Direction");
      myFile.close();
      Serial.println(F("File created on SD card."));
    } else {
      Serial.println("Error creating " + String(FILENAME));
      return false;
    }
  } else {
    Serial.println(F("File already exists on SD card."));
  }
  return true;
}

#Void setup meant to start up the connection to the amplifiers and the clock
void setup() {
  Serial.begin(9600);
  Serial.println("Adafruit MAX31865 PT100 Sensor Test!");

  if (!rtc.begin()) {
    Serial.println("Couldn't find RTC");
    while (1);
  }
//To manually adjust the time. Comment out if time is in sync
//rtc.adjust(DateTime(2023, 7, 5, 14, 53, 30));

  for(int i = 0; i < 11; i++) {
    thermo[i].begin(MAX31865_4WIRE);
  }

  pinMode(AMP_OUTPUT_PIN, INPUT);
  if (!initSDCard()) {
    while (1);
  }
}

float mapf(float x, float in_min, float in_max, float out_min, float out_max) {
  return (x - in_min) * (out_max - out_min) / (in_max - in_min) + out_min;
}

#void loop is responsible for the logging and printing of the data in the SD card.
void loop() {
  float temps[11];
  for(int i = 0; i < 11; i++) {
    temps[i] = thermo[i].temperature(RNOMINAL, RREF);
  }

  // Anemometer readings
  int rawSpeed = analogRead(ANEMOMETER_WIND_SPEED_PIN);
  int rawDirection = analogRead(ANEMOMETER_WIND_DIRECTION_PIN);
  float windSpeed = mapf(rawSpeed, 0, 1023, 0, 32.4);
  float windDirection = mapf(rawDirection, 0, 1023, 0, 359);

  // Pyranometer readings
  int sensorValue = analogRead(AMP_OUTPUT_PIN);
  float voltage = sensorValue * (V_REF / ADC_MAX);
  float irradiance = mapf(voltage, 1.73, 5.0, 0.0, 1600.0);

  total = total - readings[readIndex];
  readings[readIndex] = irradiance;
  total = total + readings[readIndex];
  readIndex = readIndex + 1;
  if (readIndex >= numReadings) {
    readIndex = 0;
  }
  average = total / numReadings;

  myFile = SD.open(FILENAME, FILE_WRITE);

  if (myFile) {
    DateTime now = rtc.now();
```

```
    String dateTimeStr = String(now.year()) + "-" + String(now.month()) + "-" + String(now.day())
    + " " +
                         String(now.hour()) + ":" + String(now.minute()) + ":" + String(now.second
    ());

    Serial.println(dateTimeStr + " Temp: " + temps[0] + ", " + temps[1] + ", " + temps[2] + ", " +
                   temps[3] + ", " + temps[4] + ", " + temps[5] + ", " + temps[6] + ", " + temps
    [7] + ", " + temps[8] + ", " + temps[9] + ", " + temps[10] +
                   " Voltage: " + voltage +
                   " Irradiance: " + average +
                   " Wind Speed: " + windSpeed + " m/s, " +
                   " Wind Direction: " + windDirection + " deg");

    myFile.println(dateTimeStr + ", " + temps[0] + ", " + temps[1] + ", " + temps[2] + ", " +
                   temps[3] + ", " + temps[4] + ", " + temps[5] + ", " + temps[6] + ", " + temps
    [7] + ", " + temps[8] + ", " + temps[9] + ", " + temps[10] +
                   ", " + voltage + ", " + average + ", " + windSpeed + ", " + windDirection);
    myFile.close();
  } else {
    Serial.println("Error opening arduino2.csv for writing. Trying to reinitialize SD card...");
    if (!initSDCard()) {
      Serial.println("Failed to reinitialize SD card. Will try again in the next loop iteration.")
    ;
    }
  }

  delay(4000);
}
}
```

Appendix H

Appendix - EnviMet

EnviMet is an Urban climate simulation software meant to analyze the microclimate on various scales, from buildings to an entire city. The initial intention with this software was to model roofs with different properties compared to the ones where the measurement campaign took place. To analyze the impact of different roofing materials on the microclimate and incorporate this knowledge into the prediction tool. Unfortunately, due to the computational limit of the Student version, any attempt to conclude a successful simulation was hindered. Various models with different scales were created to attempt to conclude the analysis but all the attempts were plagued with errors. The following models were made in EnviMet:

Figure H.1: Large scale model of TMV

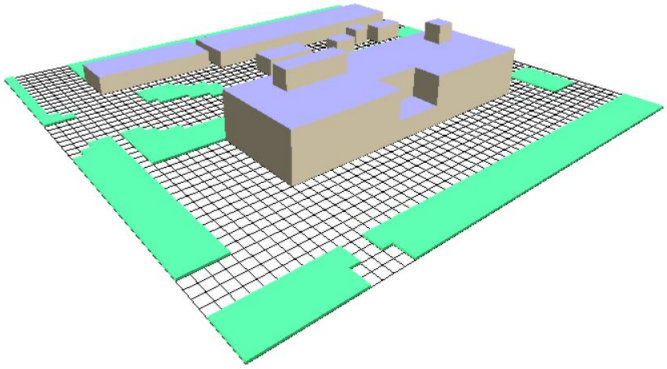

Figure H.2: Large scale model of PON

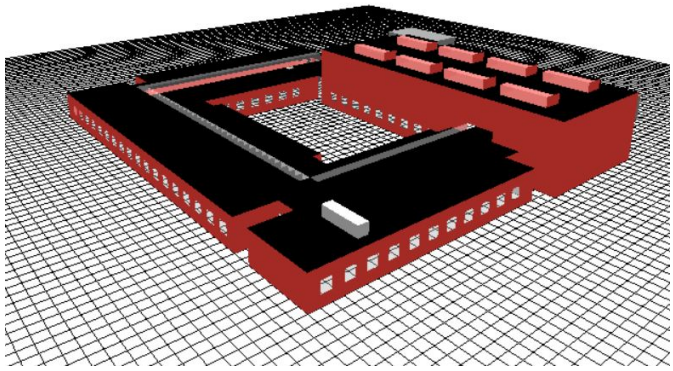

Figure H.3: Small scale model of the HVAC unit located at PON